SUPPORTING INFORMATION

Targeted Catalytic Inactivation of Angiotensin Converting Enzyme by Lisinopril-Coupled Transition Metal Chelates

Jeff C. Joyner,[1,2] Lalintip Hocharoen,[1] and J. A. Cowan[1,2,3]*

Contribution from [1] Evans Laboratory of Chemistry, Ohio State University, 100 West 18th Avenue, Columbus, Ohio 43210; [2] The Ohio State Biochemistry Program, 784 Biological Sciences 484 W. 12th Avenue, Columbus, Ohio 43210; and [3] MetalloPharm LLC, 1790 Riverstone Drive, Delaware, OH 43015

Correspondence to: Dr. J. A. Cowan, Evans Laboratory of Chemistry, Ohio State University, 100 West 18th Avenue, Columbus, Ohio 43210. tel: 614-292-2703, e-mail: cowan@chemistry.ohio-state.edu

Table of Contents for Supporting Information

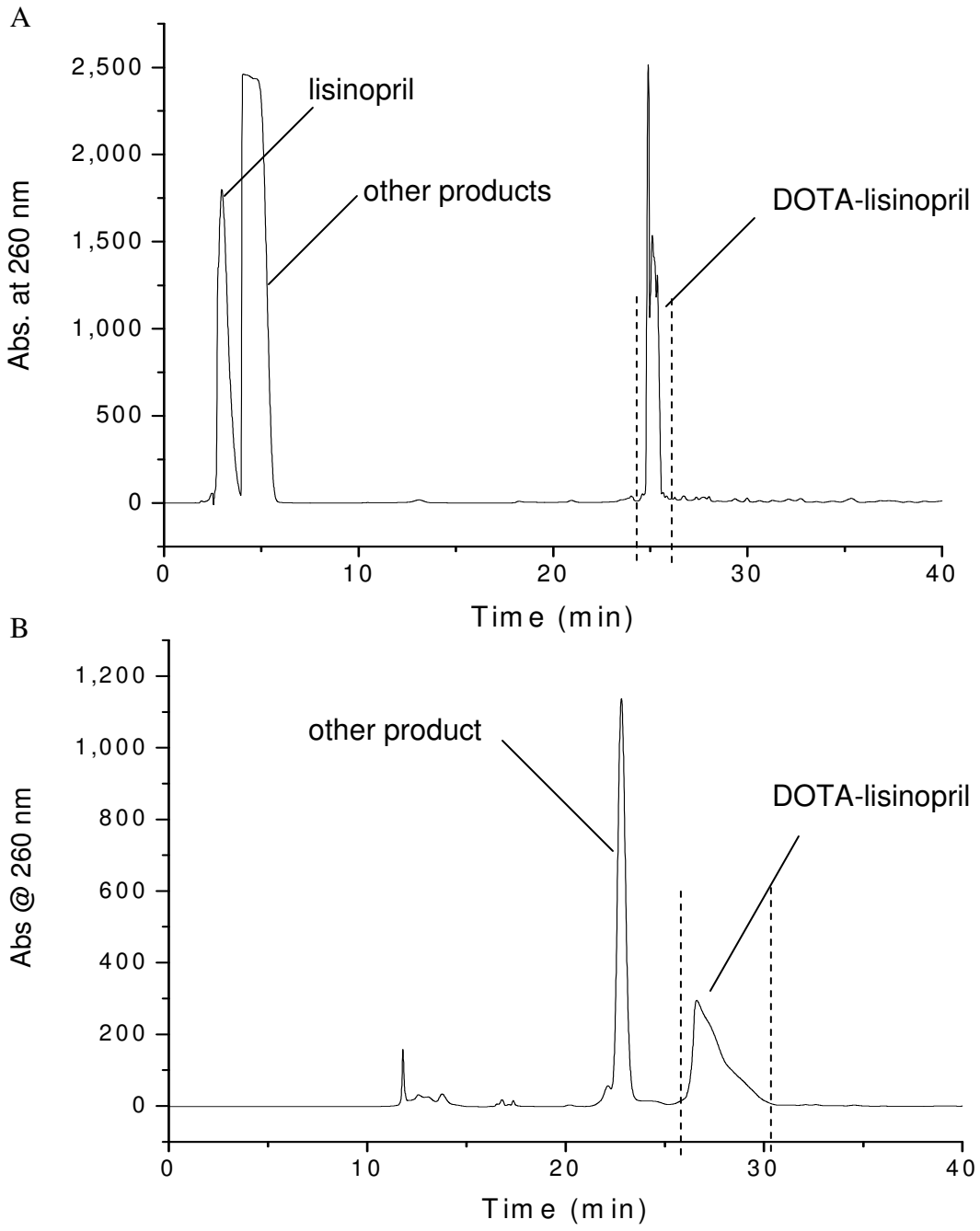

Figure SM1. Post-synthesis purification of product DOTA-lisinopril. The reaction mixture was first subject to (A) anion exchange HPLC. The fraction containing DOTA-lisinopril was then subject to (B) RP-HPLC, where DOTA-lisinopril was separated from remaining components. Collected fractions are indicated by the time between the vertical dashed lines.

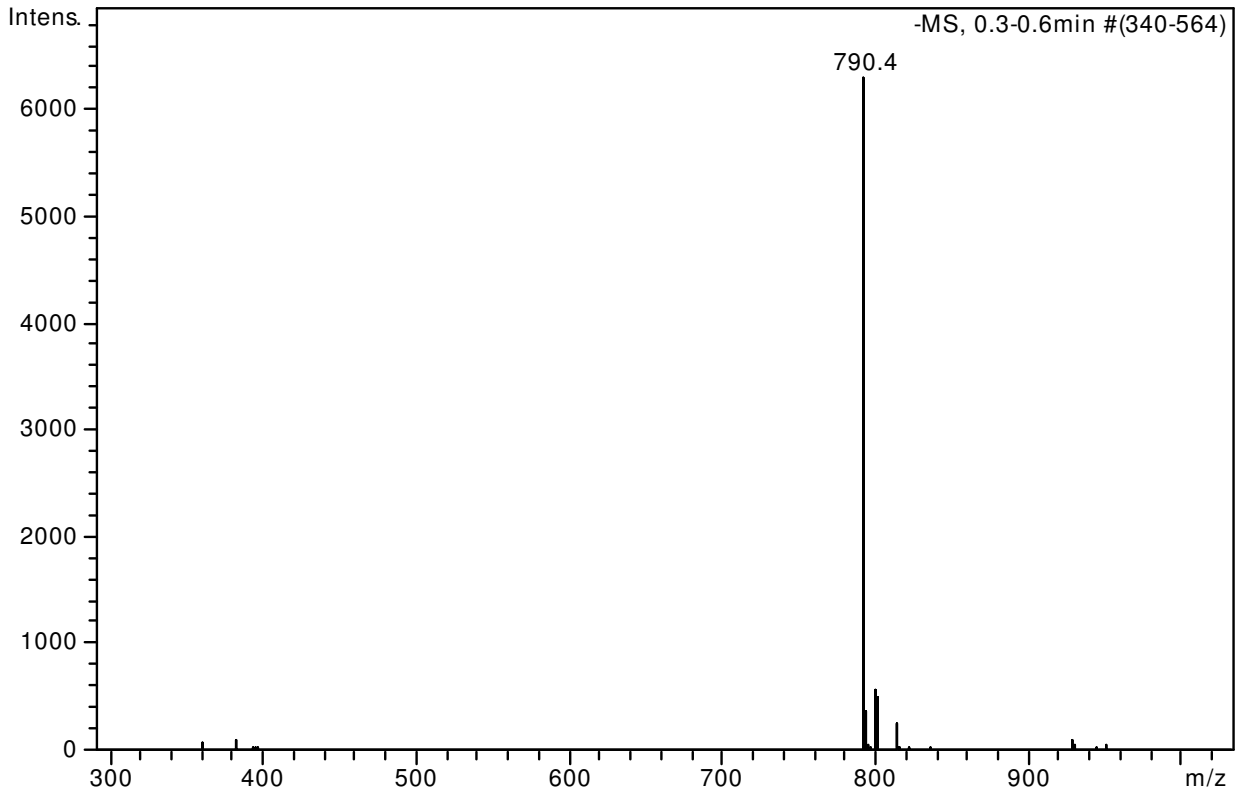

Figure SM2. ESI-MS analysis of purified DOTA-lisinopril (790 amu). No remaining uncoupled lisinopril (404 amu) was observed.

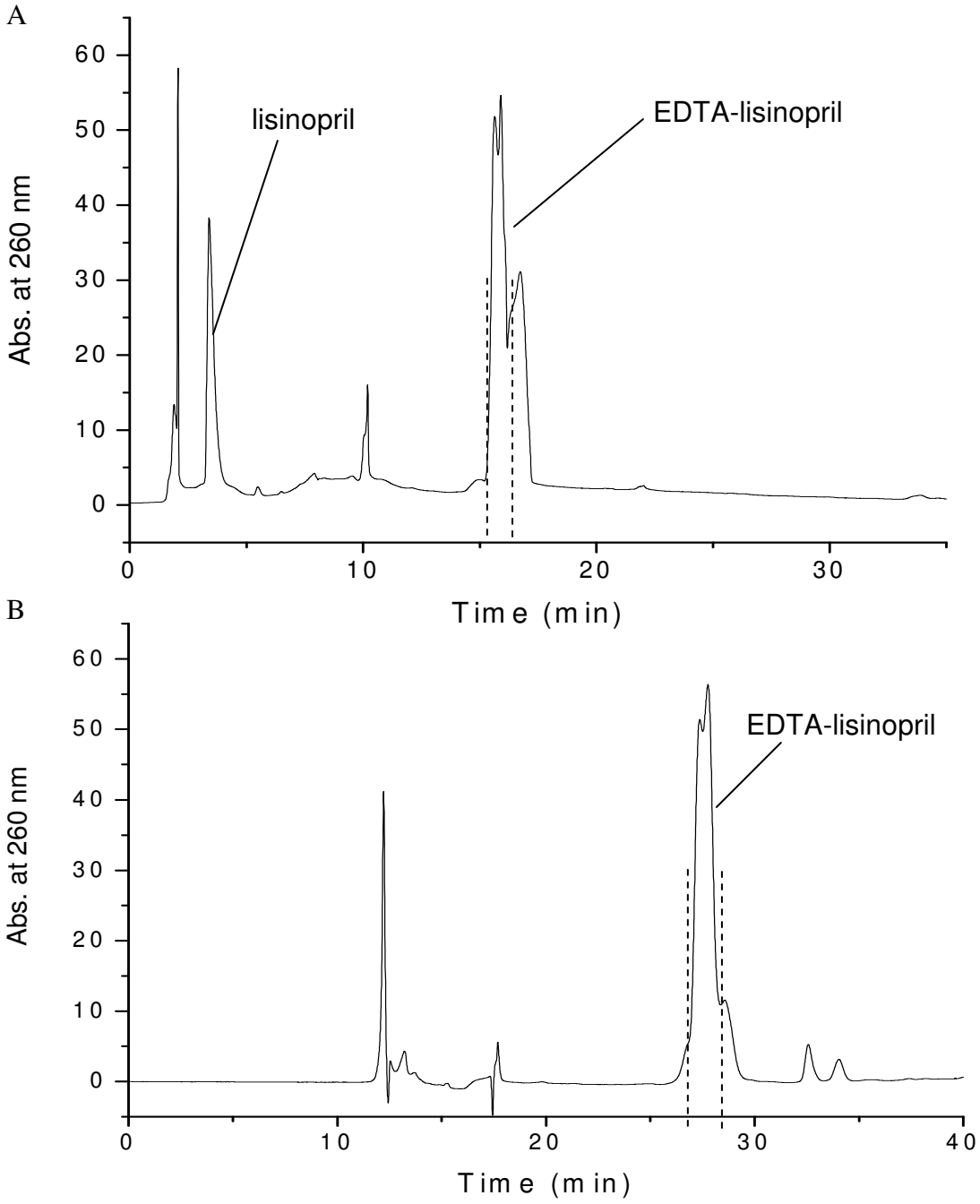

Figure SM3. Post-synthesis purification of product EDTA-lisinopril. The reaction mixture was first subject to (A) anion exchange HPLC. The fraction containing EDTA-lisinopril was then subject to (B) RP-HPLC, where EDTA-lisinopril was separated from remaining components. Collected fractions are indicated by the time between the vertical dashed lines.

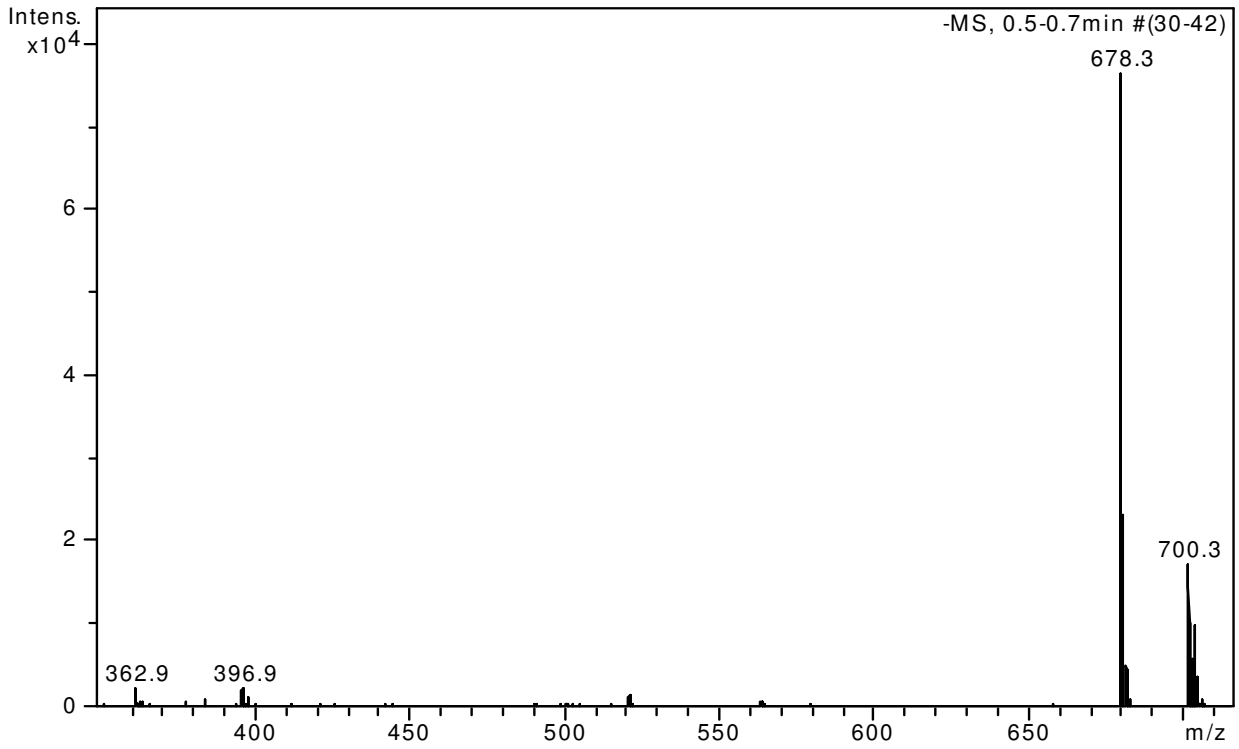

Figure SM4. ESI-MS analysis of purified EDTA-lisinopril (678 amu for $[(\text{EDTA-lisinopril})\text{-}1H^{+}]^{1-}$ and 700 amu for $[(\text{EDTA-lisinopril})\text{-}2H^{+}+1Na^{+}]^{1-}$). No remaining uncoupled lisinopril (404 amu) was observed.

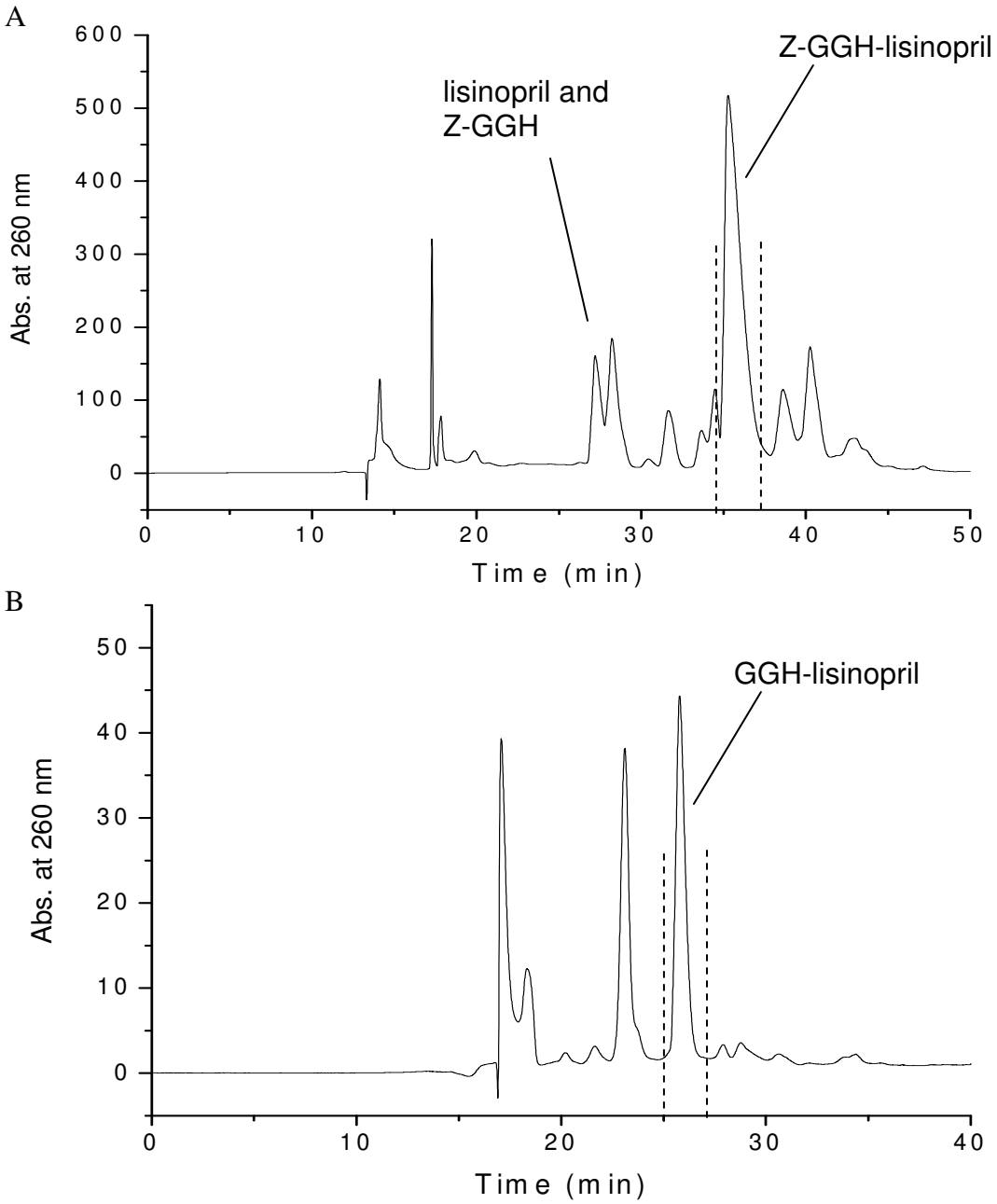

Figure SM5. Post-synthesis purification of product GGH-lisinopril. (A) Z-GGH-lisinopril was isolated by RP-HPLC (Z = carboxybenzyl). Following deprotection of Z-GGH-lisinopril to give GGH-lisinopril, (B) GGH-lisinopril was isolated by RP-HPLC. Collected fractions are indicated by the time between the vertical dashed lines.

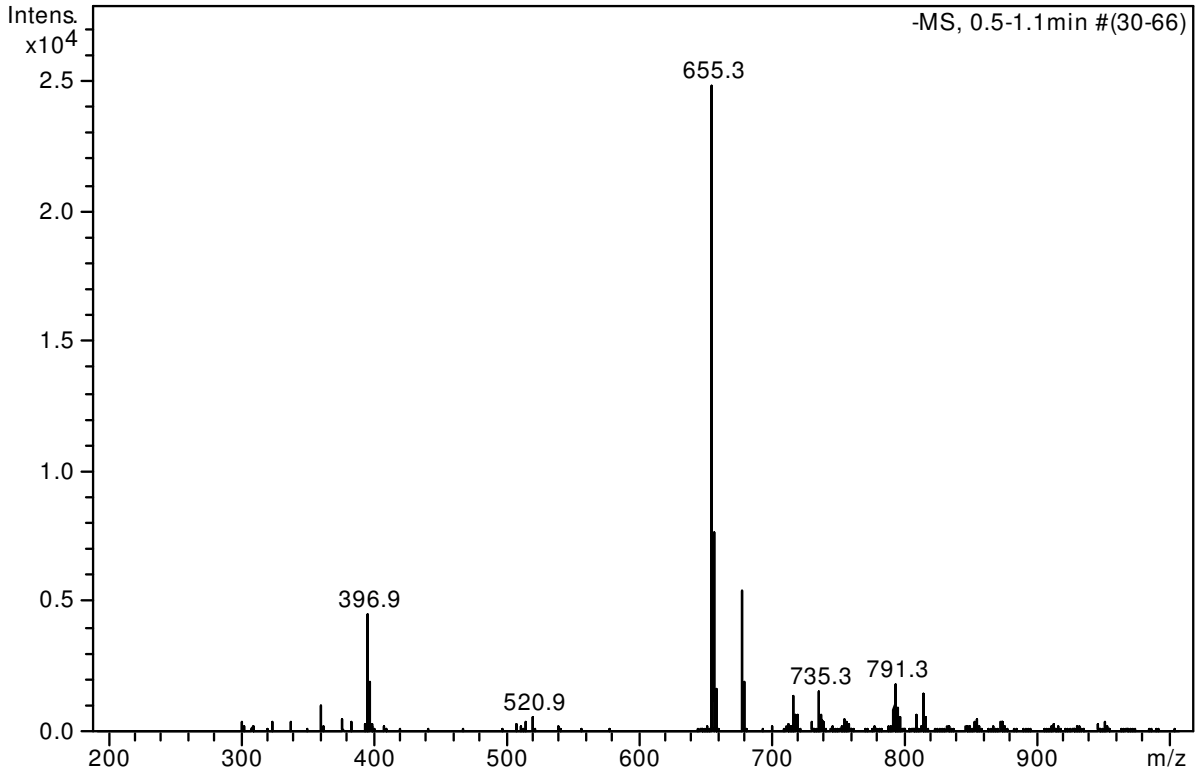

Figure SM6. ESI-MS analysis of purified GGH-lisinopril (655 amu for $[(\text{GGH-lisinopril})\text{-}1H^{+}]^{1-}$ and 677 amu for $[(\text{GGH-lisinopril})\text{-}2H^{+}+1Na^{+}]^{1-}$). No remaining uncoupled lisinopril (404 amu) was observed. Trace levels were observed for the deprotection byproduct $[(\text{Z-GGH-lisinopril}) + 2H - 1H^{+}]^{1-}$ with mass 791 amu as well as the corresponding Na^{+} adduct with mass 813 amu (where Z = carboxybenzyl). The trace peak at 713 amu appeared to be an artifactual Ni^{2+} adduct of GGH-lisinopril, and the corresponding Na^{+} adduct was also observed at 735 amu.

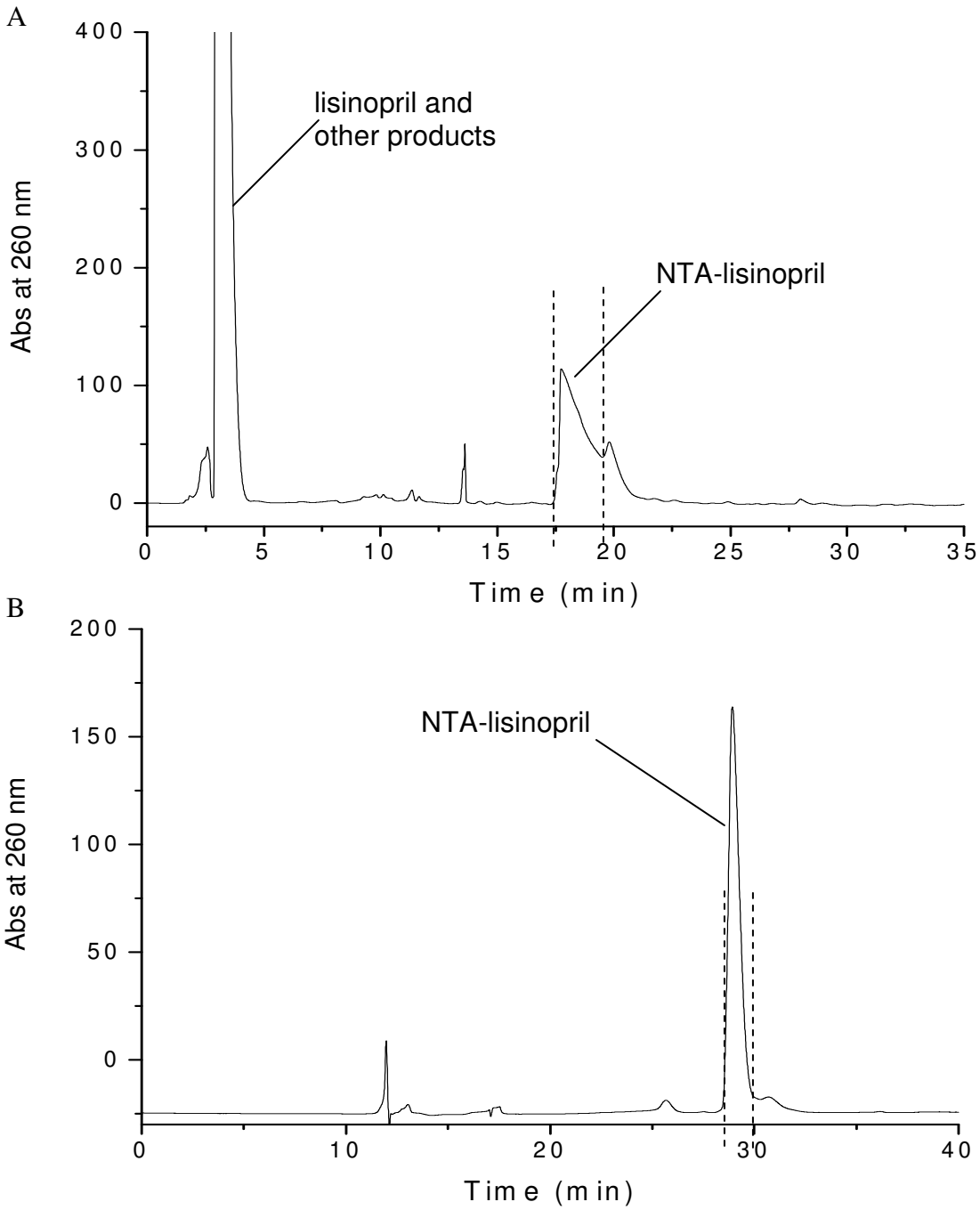

Figure SM7. Post-synthesis purification of product NTA-lisinopril. The reaction mixture was first subject to (A) anion exchange HPLC. The fraction containing NTA-lisinopril was then subject to (B) RP-HPLC, where NTA-lisinopril was separated from remaining components. Collected fractions are indicated by the time between the vertical dashed lines.

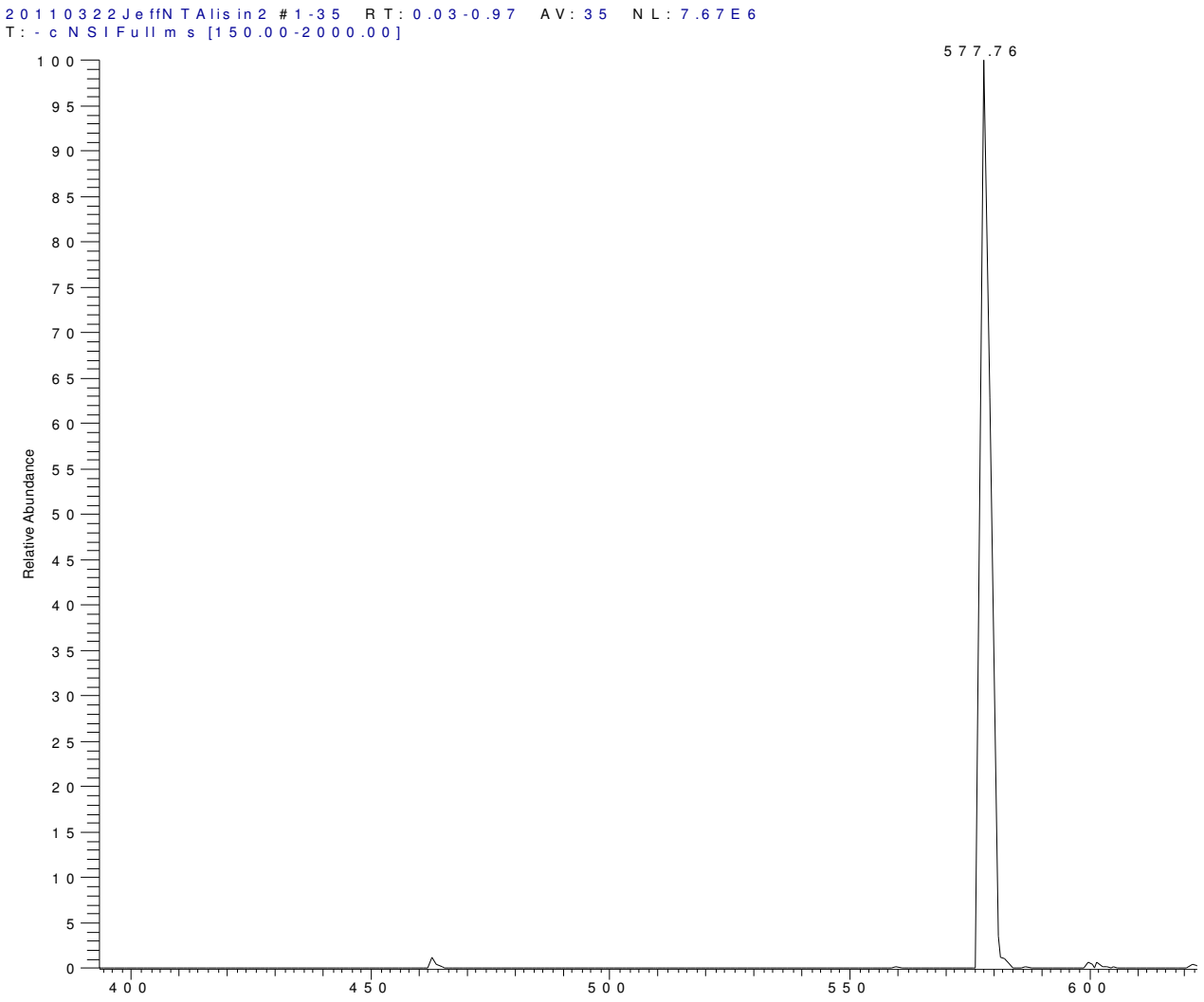

Figure SM8. ESI-MS analysis of purified NTA-lisinopril (578 amu). No remaining uncoupled lisinopril (404 amu) was observed. Data for NTA-lisinopril was obtained using an LCQ-Deca in the laboratory of Dr. Michael Freitas.

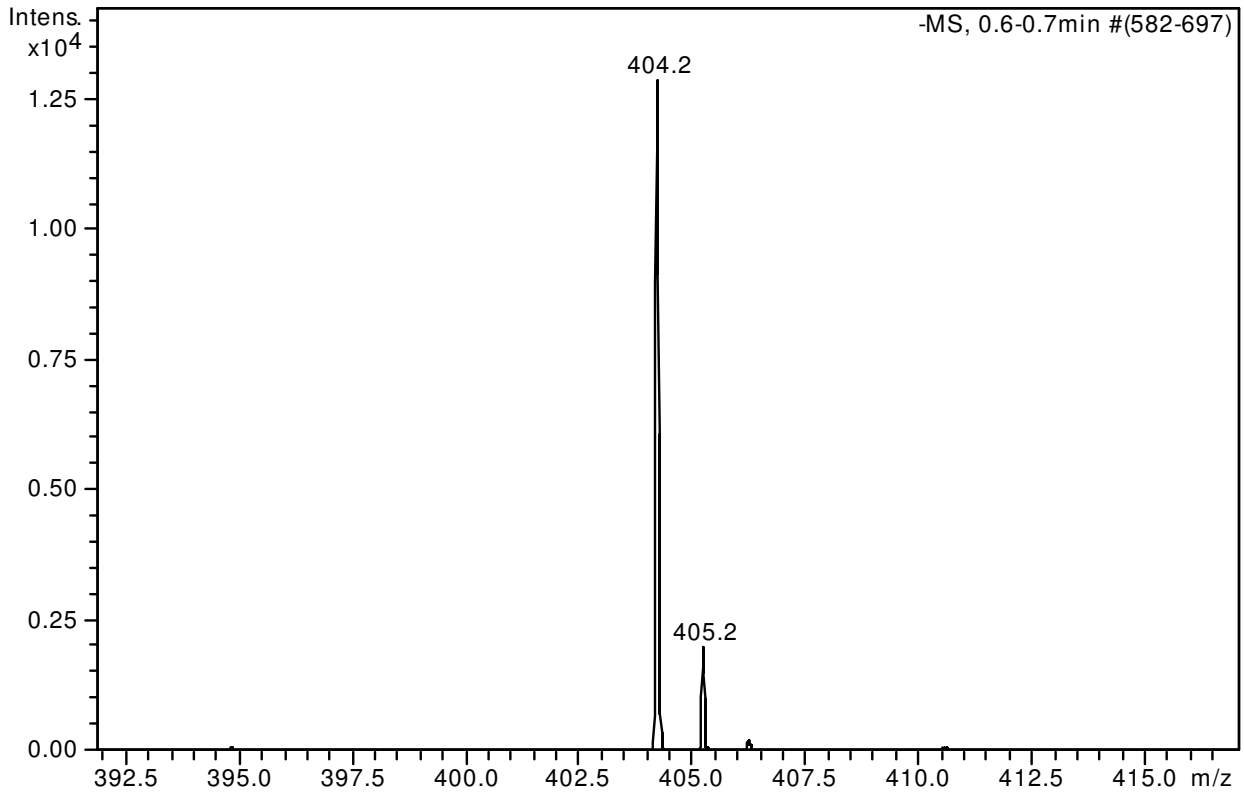

Figure SM9. ESI-MS analysis of lisinopril (404 amu).

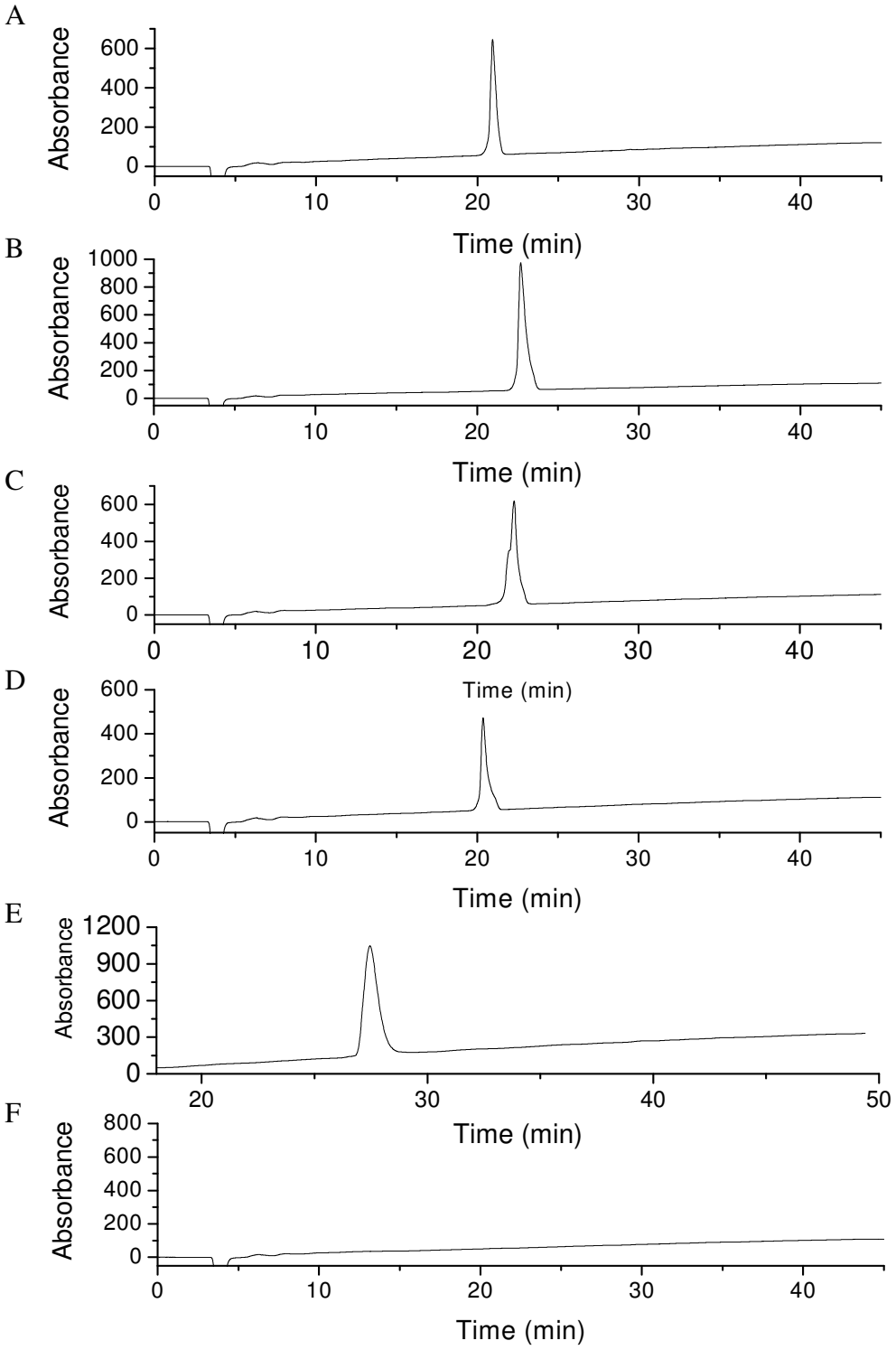

Figure SM10. RP-HPLC chromatograms of purified chelate-lisinopril products. (A) lisinopril, (B) DOTA-lisinopril, (C) EDTA-lisinopril, (D) GGH-lisinopril, (E) NTA-lisinopril, and (F) water injection. All samples were run on a VYDAC analytical C18 column (250 × 5 mm), with a gradient of 0 – 50% B over 50 min (A = water with 0.1% TFA; B = acetonitrile with 0.1% TFA), except for NTA-lisinopril, which was run on the VYDAC preparatory C18 column, using the same gradient as used for purification (described in the manuscript).

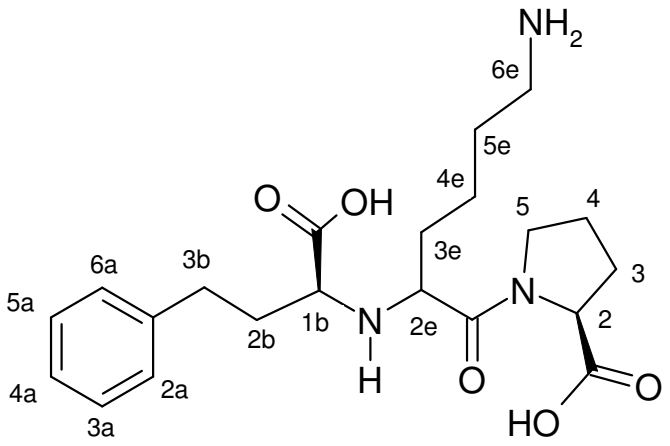

Figure SM11. Lisinopril, with ^{1}H-NMR proton labeling scheme, adapted from Sakamoto et al.[1]

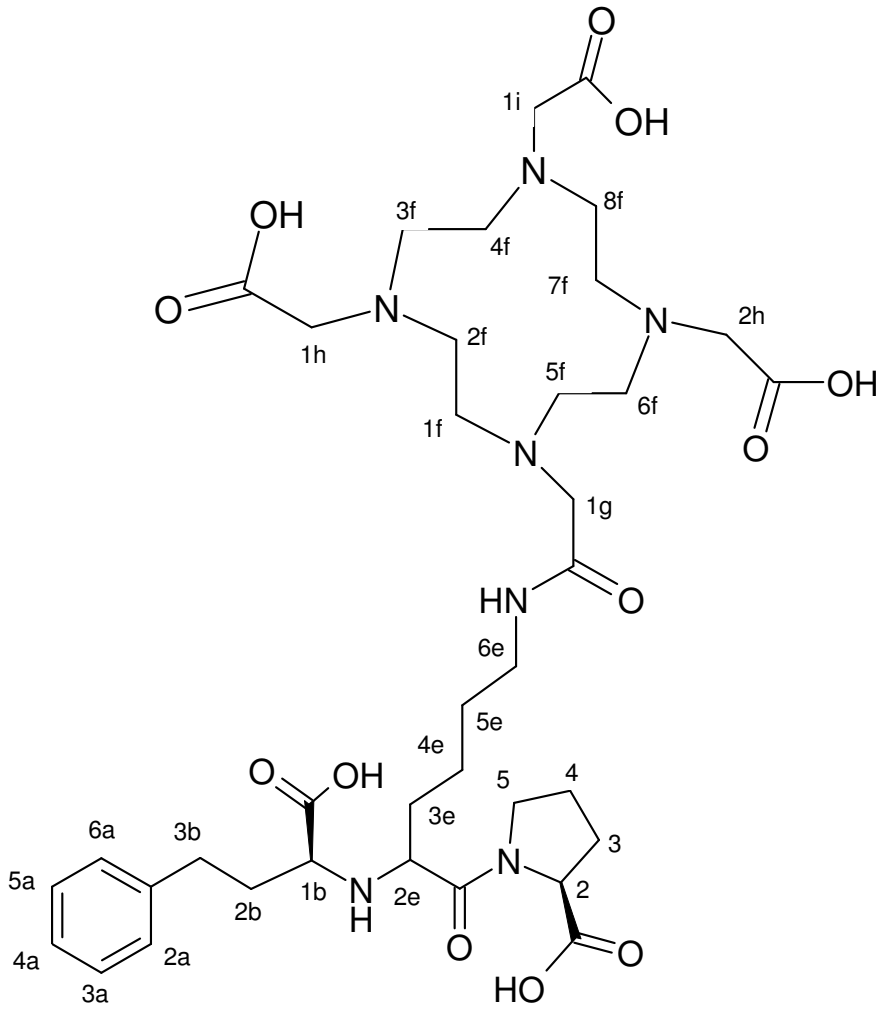

Figure SM12. DOTA-lisinopril, with ^{1}H-NMR proton labeling scheme. Labels used for the lisinopril portion are the same as used for lisinopril lacking attached chelator. Labels used for the DOTA portion are the same as used for DOTA lacking attached lisinopril. DOTA-lisinopril ^{1}H-NMR (D_2O, 500.157 MHz) δ ppm 7.35 (m, 2H), 7.27 (m, 3H), 4.41 (m, 1H), 4.23 (t, 1H), 3.75 (s, 8H, broad), 3.57 (s, 2H), 3.49 (t, 1H), 3.25 (m, 18H, broad), 2.72 (sextet, 2H), 2.28 (m, 2H), 2.17 (qr, 2H), 2.04 (s, 2H), 1.96 (m, 2H), 1.52 (qr, 2H), 1.46 (m, 2H)

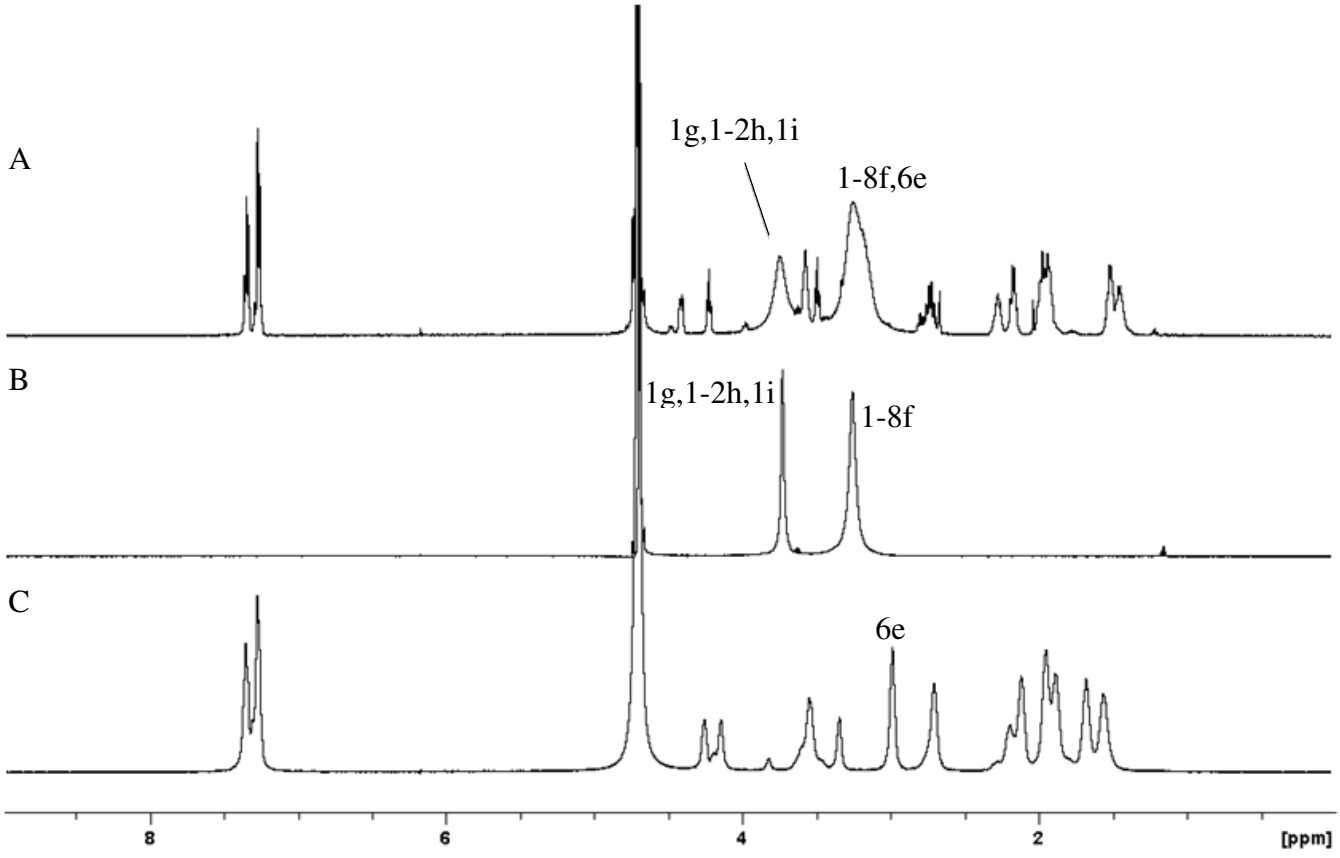

Figure SM13. ^{1}H-NMR for (A) DOTA-lisinopril, (B) DOTA, and (C) lisinopril in D_2O; the numbers of non-exchangeable protons are 50, 24, and 26, respectively. Tentative assignments for the protons 6e (2H) from lisinopril and 1-8f, 1g, 1-2h, and 1i (24H) are shown. The observed and calculated numbers of protons match for each spectrum.

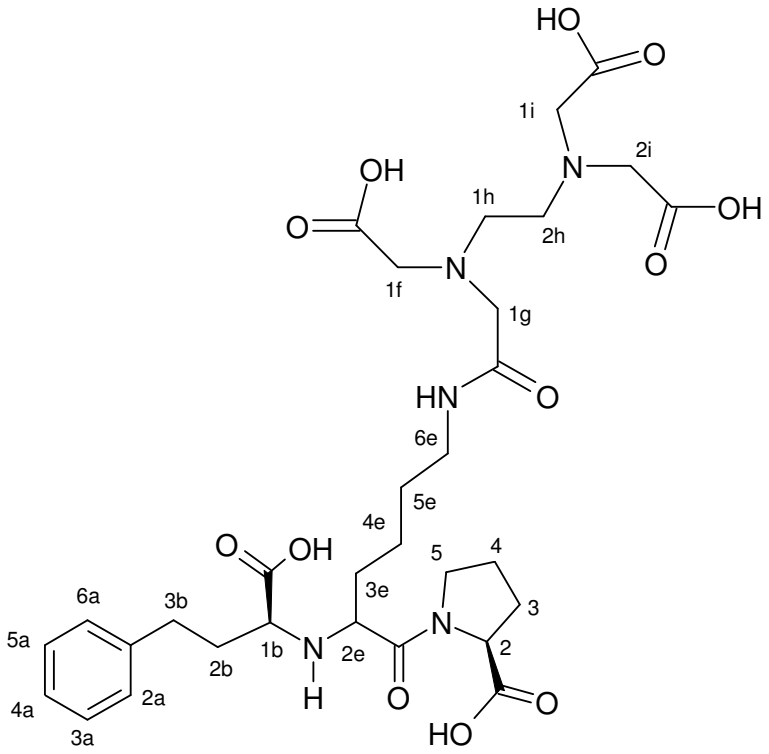

Figure SM14. EDTA-lisinopril, with ^{1}H-NMR proton labeling scheme. Labels used for the lisinopril portion are the same as used for lisinopril lacking attached chelator. Labels used for the EDTA portion are the same as used for EDTA lacking attached lisinopril. EDTA-lisinopril ^{1}H-NMR (D_2O, 500.157 MHz) δ ppm 7.35 (m, 2H), 7.28 (m, 3H), 4.41 (m, 1H), 4.22 (t, 1H), 3.89 (s, 4H), 3.66 (d, 4H), 3.61 (s, 1H), 3.57 (m, 1H), 3.47 (t, 1H), 3.41 (m, 2H), 3.23 (m, 4H), 2.73 (m, 2H), 2.27 (m, 2H), 2.16 (qr, 2H), 1.96 (m, 4H), 1.54 (m, 2H), 1.47 (m, 2H)

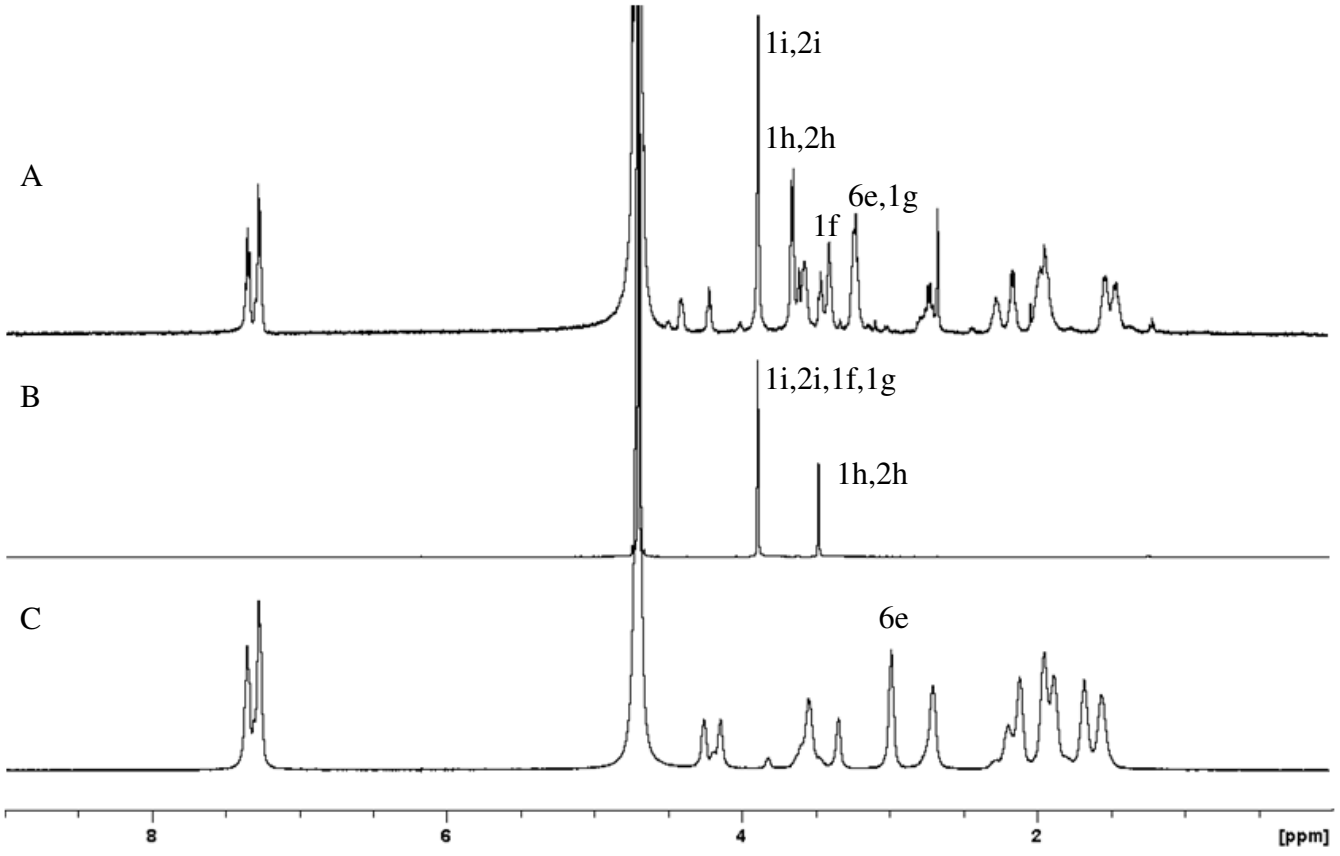

Figure SM15. ^{1}H-NMR for (A) EDTA-lisinopril, (B) EDTA, and (C) lisinopril in D_2O; the numbers of non-exchangeable protons are 38, 12, and 26, respectively. Tentative assignments for the protons 6e (2H) from lisinopril and 1i, 2i, 1f, 1g, 1h, 2h (12H) from EDTA are shown. The observed and calculated numbers of protons match for each spectrum. A residual DMSO peak was observed at ~ 2.7 ppm.

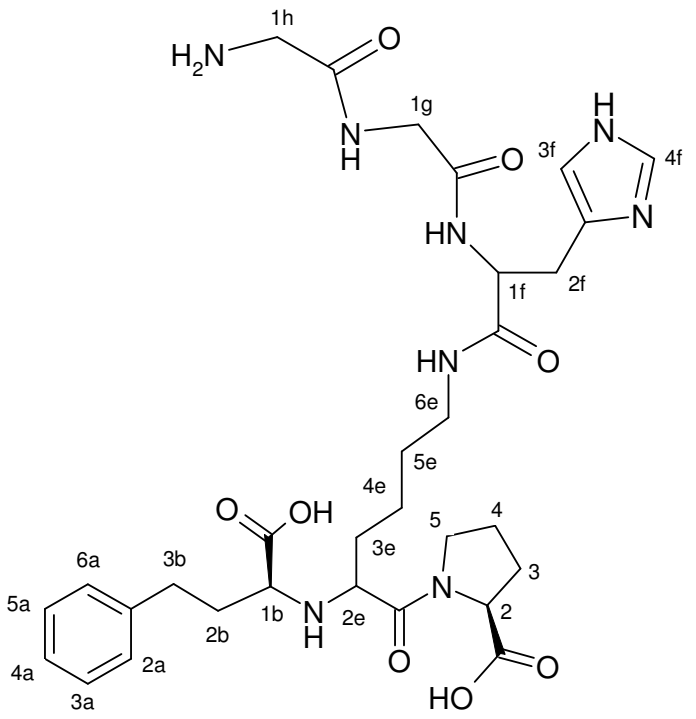

Figure SM16. GGH-lisinopril, with ^{1}H-NMR proton labeling scheme. Labels used for the lisinopril portion are the same as used for lisinopril lacking attached chelator. Labels used for the GGH portion are the same as used for GGH lacking attached lisinopril. GGH-lisinopril ^{1}H-NMR (D_2O, 500.157 MHz) δ ppm 8.58 (m, 1H), 7.35 (m, 2H), 7.27 (m, 3H + 1H), 4.62 (m, 1H), 4.41 (m, 1H), 4.20 (t, 1H), 3.94 (s, 2H), 3.87 (s, 2H), 3.56 (qr, 2H), 3.49 (t, 1H), 3.16 (t, 2H), 3.16 (d of qr, 2H), 2.73 (sextet, 2H), 2.28 (t, 2H), 2.17 (qr, 2H), 1.93 (m, 4H), 1.43 (m, 4H)

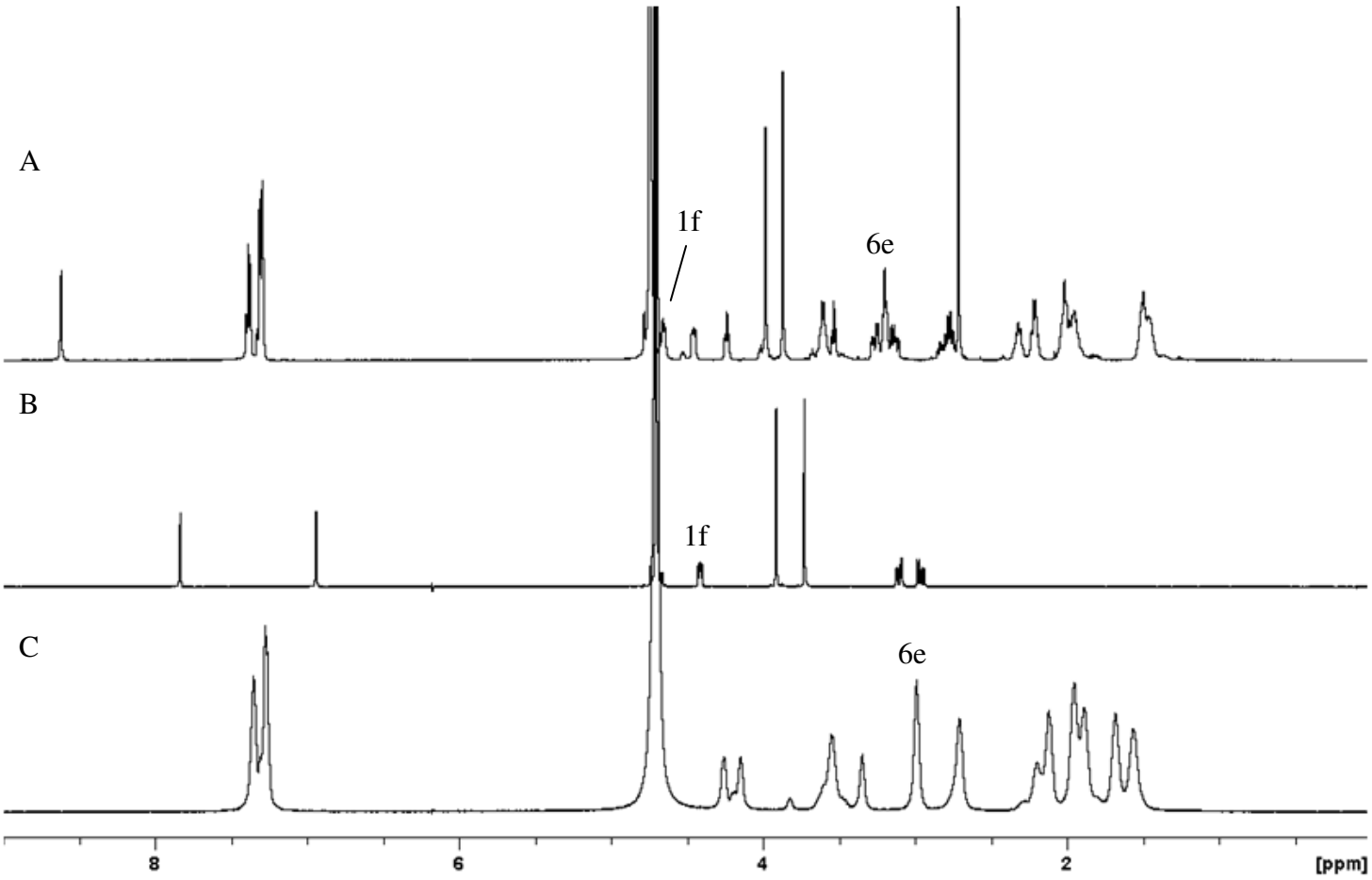

Figure SM17. ^{1}H-NMR for (A) GGH-lisinopril, (B) GGH, and (C) lisinopril in D_2O; the numbers of non-exchangeable protons are 35, 9, and 26, respectively. Tentative assignments for the protons 6e (2H) from lisinopril and 1f (1H) from GGH are shown. The observed and calculated numbers of protons match for each spectrum. A residual DMSO peak was observed at ~ 2.7 ppm.

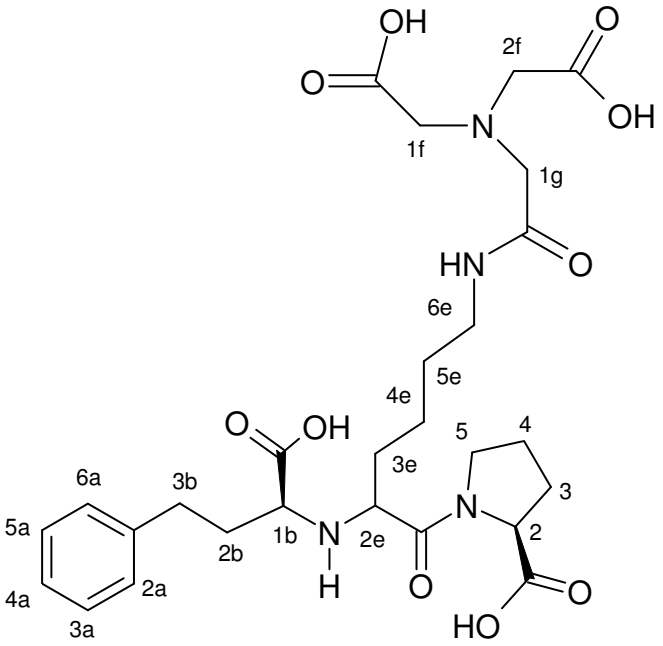

Figure SM18. NTA-lisinopril, with ^{1}H-NMR proton labeling scheme. Labels used for the lisinopril portion are the same as used for lisinopril lacking attached chelator. Labels used for the NTA portion are the same as used for NTA lacking attached lisinopril. NTA-lisinopril ^{1}H-NMR (D_2O, 500.157 MHz) δ ppm 7.35 (m, 2H), 7.28 (m, 3H), 4.42 (m, 1H), 4.22 (t, 1H), 4.07 (s, 2H), 3.93 (s, 4H), 3.57 (s, 2H). 3.49 (t, 1H), 3.25 (t, 2H), 2.74 (m, 2H), 2.28 (m, 2H), 2.18 (qr, 2H), 2.00 (m, 4H), 1.53 (qr, 2H), 1.46 (m, 2H)

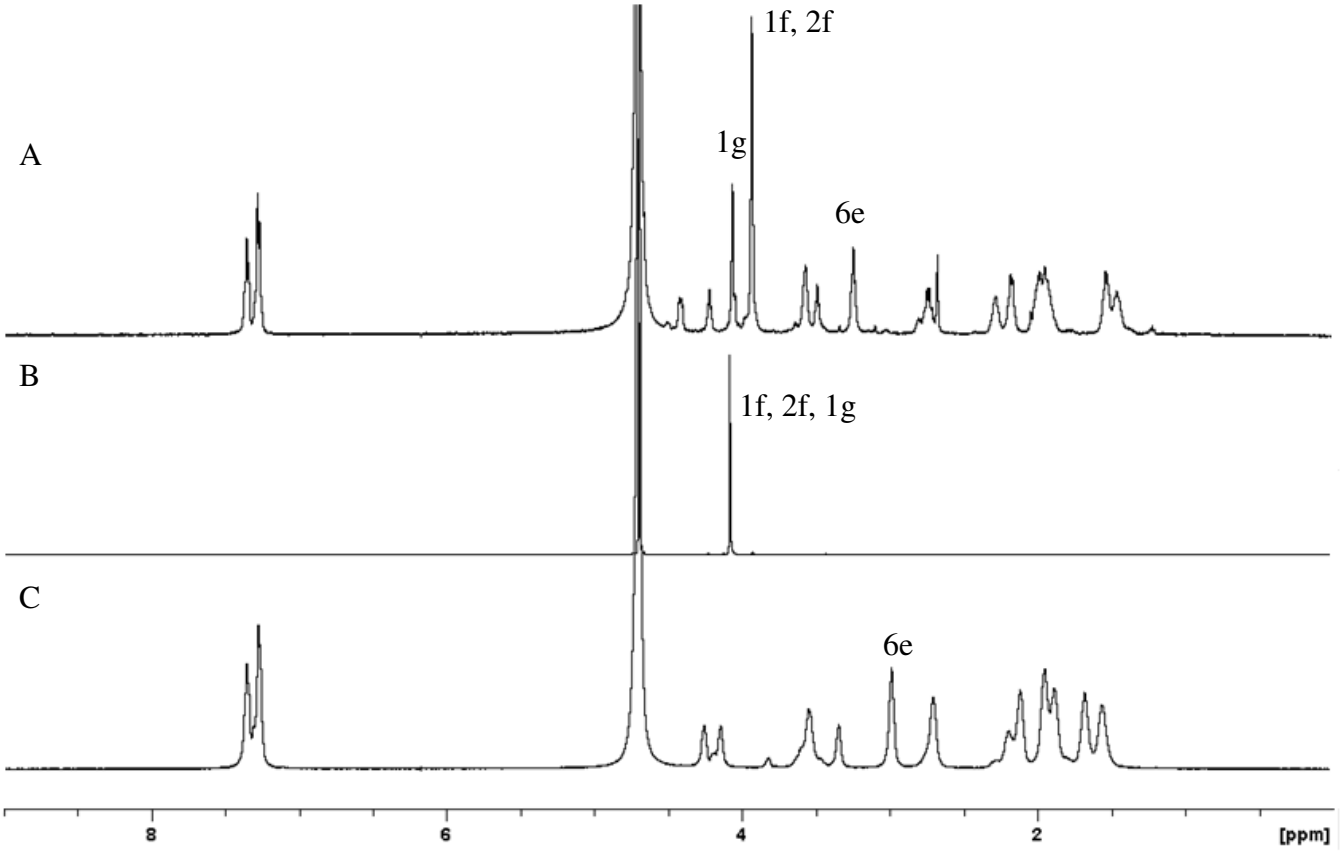

Figure SM19. ^{1}H-NMR for (A) NTA-lisinopril, (B) NTA, and (C) lisinopril in D_2O; the numbers of non-exchangeable protons are 32, 6, and 26, respectively. Tentative assignments for the protons 6e (2H) from lisinopril and 1f, 2f, and 1g (6H) from NTA are shown. The observed and calculated numbers of protons match for each spectrum. A residual DMSO peak was observed at ~ 2.7 ppm.

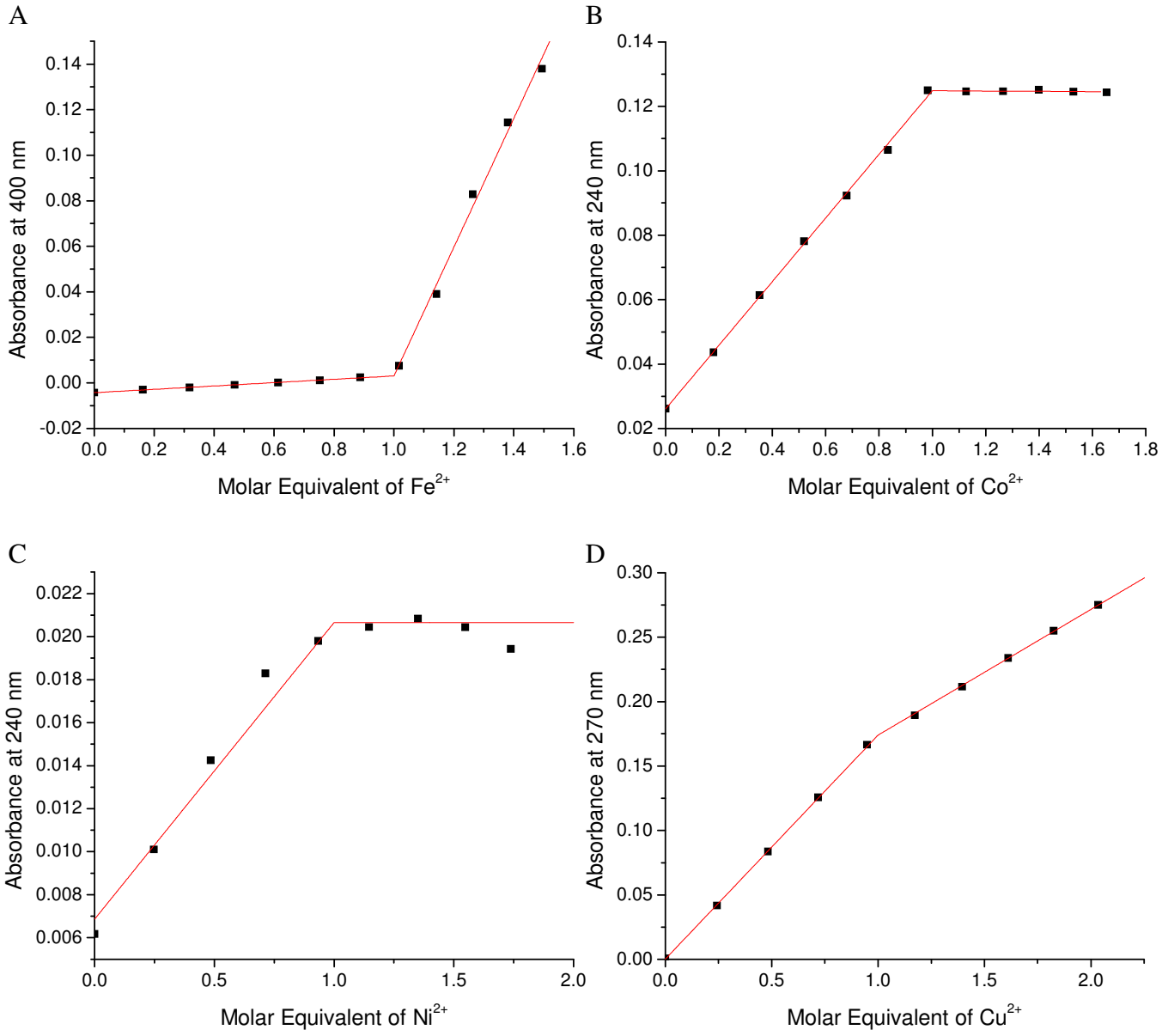

Figure SM20. UV/vis-monitored titrations of DOTA-lisinopril with (A) Fe^{2+}, (B) Co^{2+}, (C) Ni^{2+}, and (D) Cu^{2+}, performed in 20 mM HEPES, 100 mM NaCl, pH 7.4.

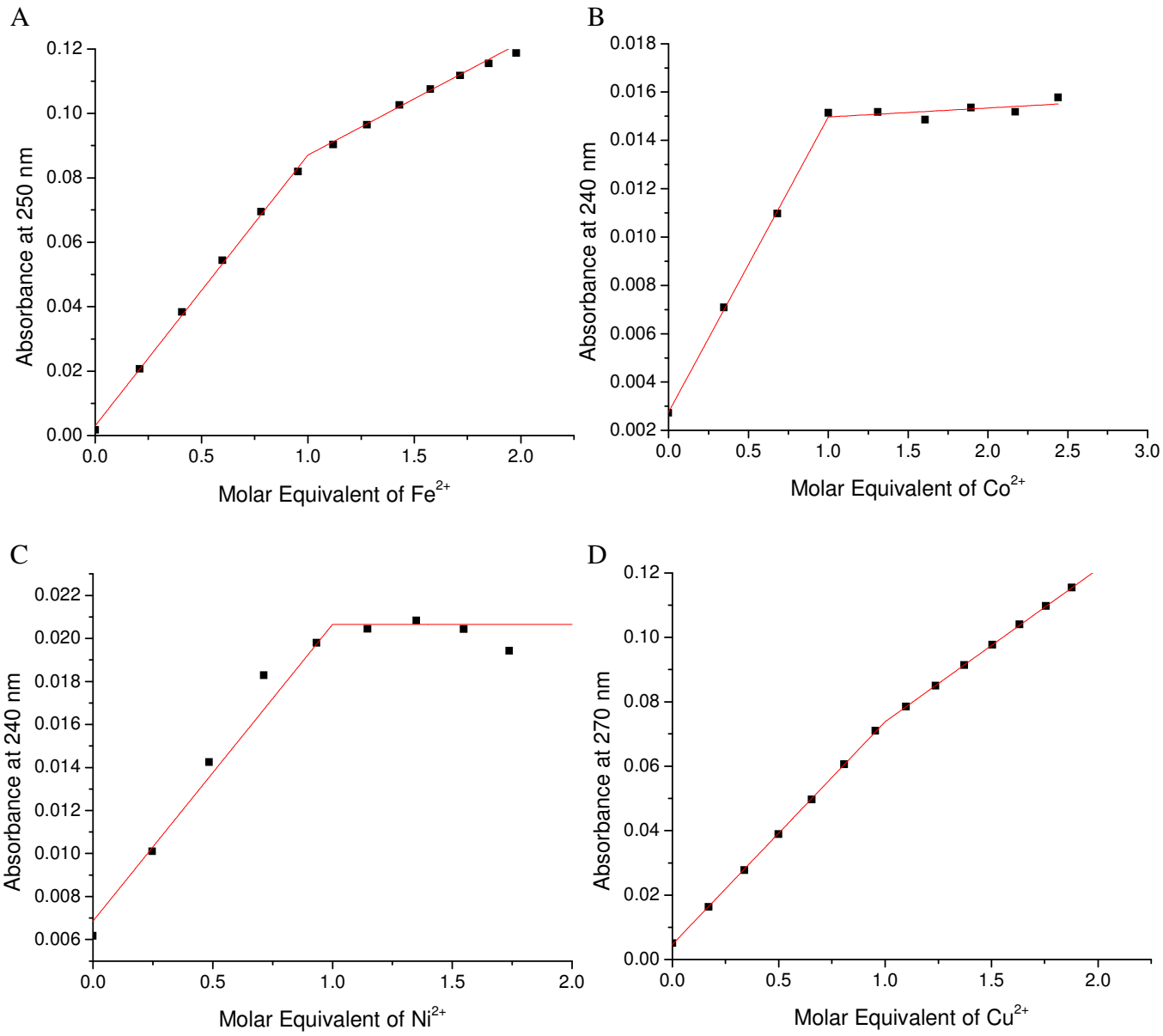

Figure SM21. UV/vis-monitored titrations of EDTA-lisinopril with (A) Fe^{2+}, (B) Co^{2+}, (C) Ni^{2+}, and (D) Cu^{2+}, performed in 20 mM HEPES, 100 mM NaCl, pH 7.4.

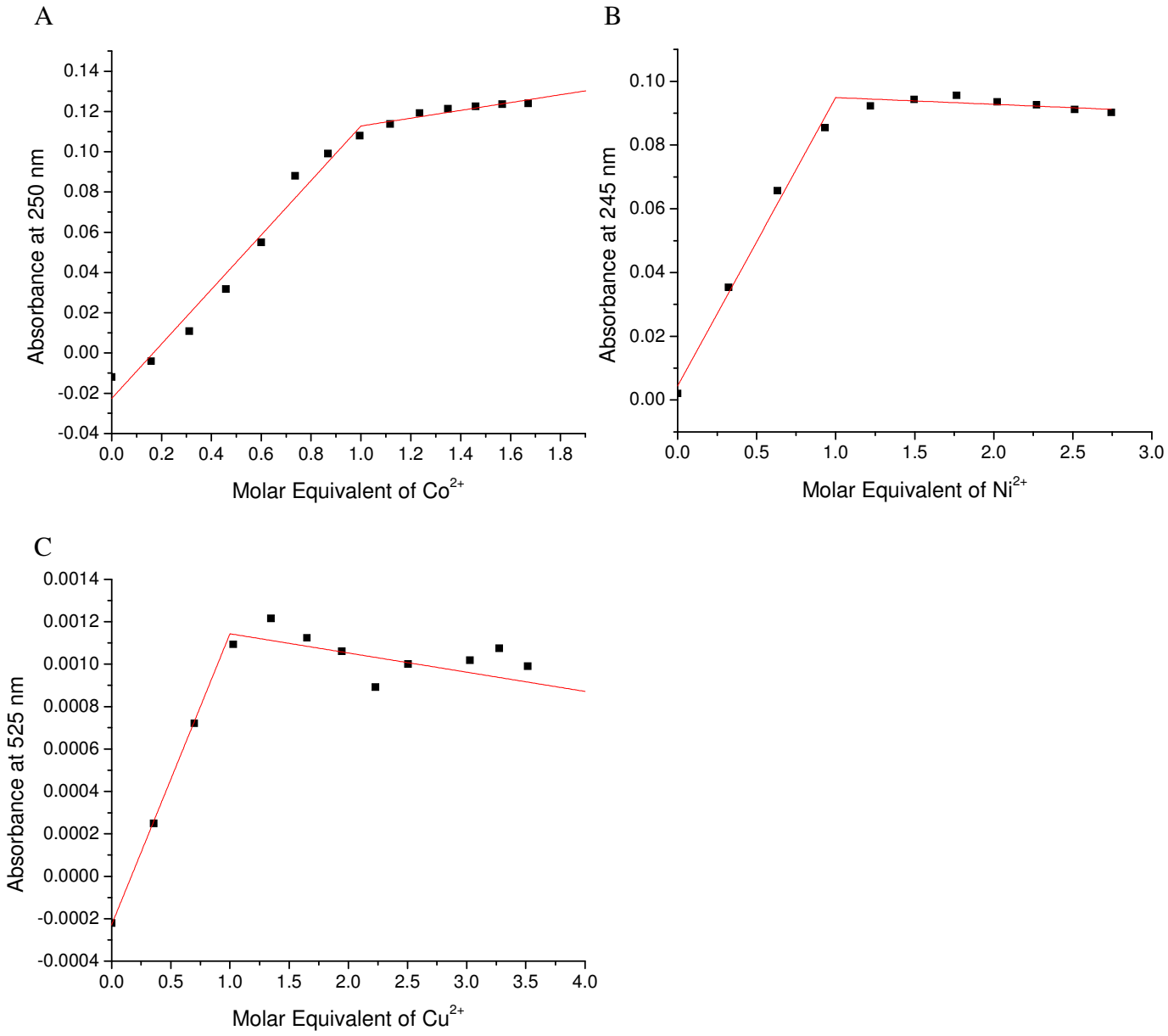

Figure SM22. UV/vis-monitored titrations of GGH-lisinopril with (A) Co^{2+}, (B) Ni^{2+}, and (C) Cu^{2+}, performed in 20 mM HEPES, 100 mM NaCl, pH 7.4.

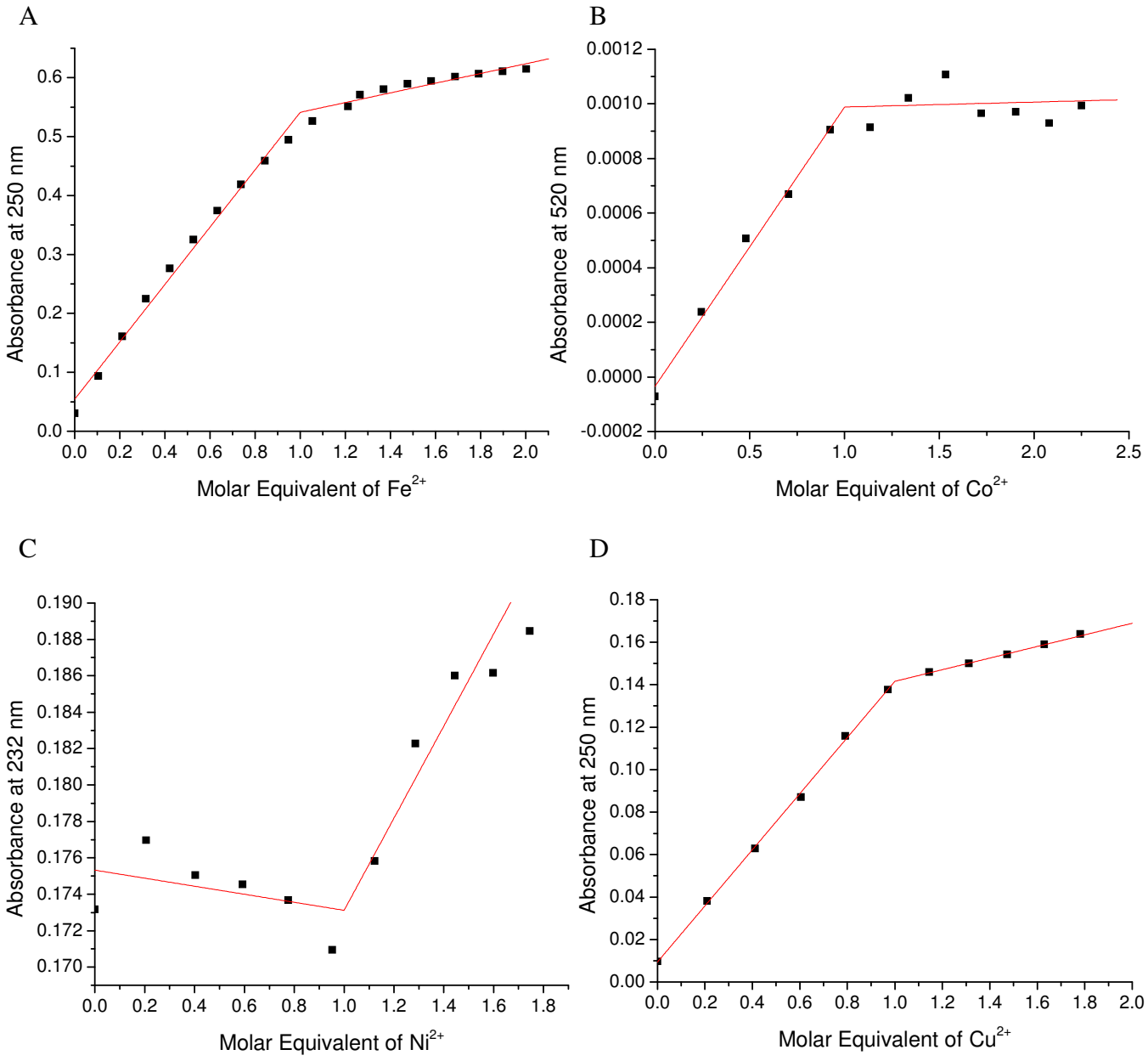

Figure SM23. UV/vis-monitored titrations of NTA-lisinopril with (A) Fe^{2+}, (B) Co^{2+}, (C) Ni^{2+}, and (D) Cu^{2+}, performed in 20 mM HEPES, 100 mM NaCl, pH 7.4.

Complex	ε_1 ($M^{-1}cm^{-1}$)	λ_1 (nm)	ε_2 ($M^{-1}cm^{-1}$)	λ_2 (nm)
Cu-DOTA-lisinopril	4,300 ± 100	270	82 ± 3	720
Ni-DOTA-lisinopril	3,100 ± 200	240		
Co-DOTA-lisinopril	1,810 ± 90	240		
Fe-DOTA-lisinopril	60 ± 1	400		
Cu-EDTA-lisinopril	3,010 ± 30	270	80 ± 9	730
Ni-EDTA-lisinopril	380 ± 50	240		
Co-EDTA-lisinopril	720 ± 50	240		
Fe-EDTA-lisinopril	7,600 ± 400	250		
Cu-GGH-lisinopril	4,000 ± 400	250	120 ± 20	525
Ni-GGH-lisinopril	7,000 ± 1,000	245	50 ± 20	430
Co-GGH-lisinopril	2,200 ± 600	250		
Cu-NTA-lisinopril	5,600 ± 200	250	0 ± 10	700
Ni-NTA-lisinopril	< 100	232		
Co-NTA-lisinopril	330 ± 20	240	26 ± 4	520
Fe-NTA-lisinopril	7,200 ± 400	250		
lisinopril	190 ± 1	260		

Table SM1. Summary of the experimentally determined extinction coefficients (ε) at specific wavelengths (λ) for the metal-chelate-lisinopril complexes studied. Extinction coefficients were determined from linear fits of absorbance vs. metal-chelate-lisinopril concentration. Absorbance by chelate-lisinopril (primarily due to the internal phenyl and amide functional groups) was subtracted from the absorbance by the metal-chelate-lisinopril complexes, so that the reported extinction coefficients reflect only the metal chelate portion of the metal-chelate-lisinopril complexes, allowing comparison of the extinction coefficients of the metal-chelate-lisinopril complexes with the respective metal chelates lacking lisinopril.

Complex	ε_1 ($M^{-1}cm^{-1}$)	λ_1 (nm)	ε_2 ($M^{-1}cm^{-1}$)	λ_2 (nm)	log (β) of M^{2+}-chelate
Cu-DOTA	3,700 ± 20	270	99 ± 5	720	22.3[a]
Ni-DOTA	4,610 ± 20	240			20[a]
Co-DOTA	1,858 ± 8	240			20.2[a]
Fe-DOTA	164 ± 6	400			20.22[b]
Cu-EDTA	3,300 ± 100	270	100 ± 10	730	18.8[c]
Ni-EDTA	330 ± 30	240			18.56[c]
Co-EDTA	700 ± 60	240			16.03[d]
Fe-EDTA	8,900 ± 300	250			14.3[c]
Cu-GGH	4,180 ± 60	250	108 ± 5	525	15.9[e]
Ni-GGH	10,900 ± 300	245	170 ± 40	430	16[f]
Co-GGH	2,500 ± 50	250			> 7[g]
Cu-NTA	2,790 ± 80	250	50 ± 2	700	12.68[c]
Ni-NTA	200 ± 100	232			11.26[c]
Co-NTA	440 ± 40	240	30 ± 2	520	10.6[c]
Fe-NTA	6,700 ± 100	250			8.84[c]

Table SM2. Summary of the experimentally determined extinction coefficients (ε) at specific wavelengths (λ) and stability constants (β) for the metal chelates studied. Extinction coefficients were determined from linear fits of absorbance vs. metal chelate concentration. [a] Anderegg et al. (2005).[2] [b] Martell et al. (1996).[3] [c] Furia (1972).[4] [d] Ogino et al. (1983).[5] [e] Lau et al. (1974).[6] [f] Long et al. (1999).[7] [g] Determined by metal titration, monitored by absorbance at the specified wavelength; this technique provided a lower limit for the stability constant.

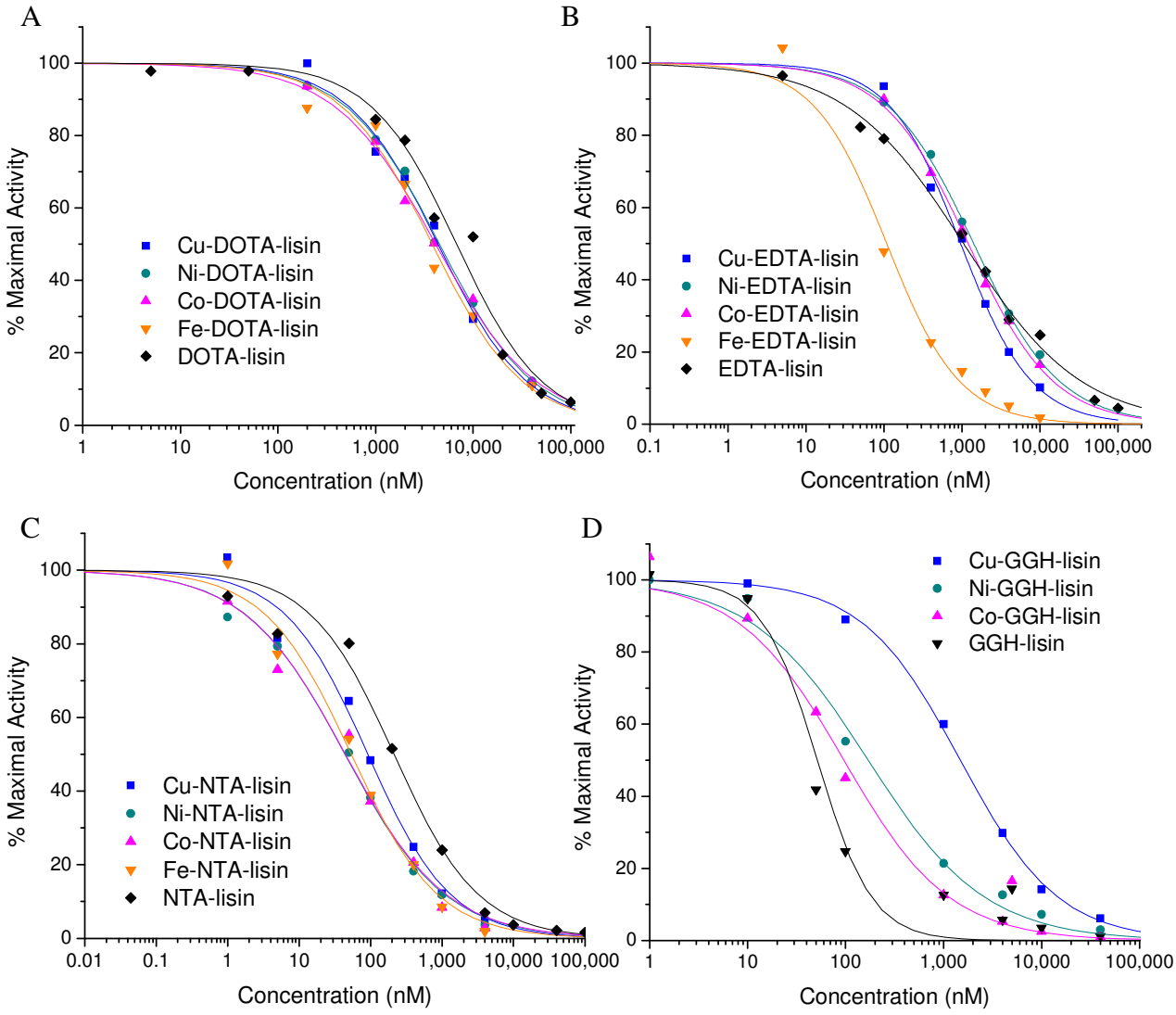

Figure SM24. Concentration-dependent inhibition of sACE-1 by metal-chelate-lisinopril complexes of Fe^{3+}, Co^{2+}, Ni^{2+}, and Cu^{2+}, and chelate-lisinopril compounds, from which IC_{50} values were obtained. (A) M-DOTA-lisinopril; (B) M-EDTA-lisinopril; (C) M-NTA-lisinopril; (D) M-GGH-lisinopril.

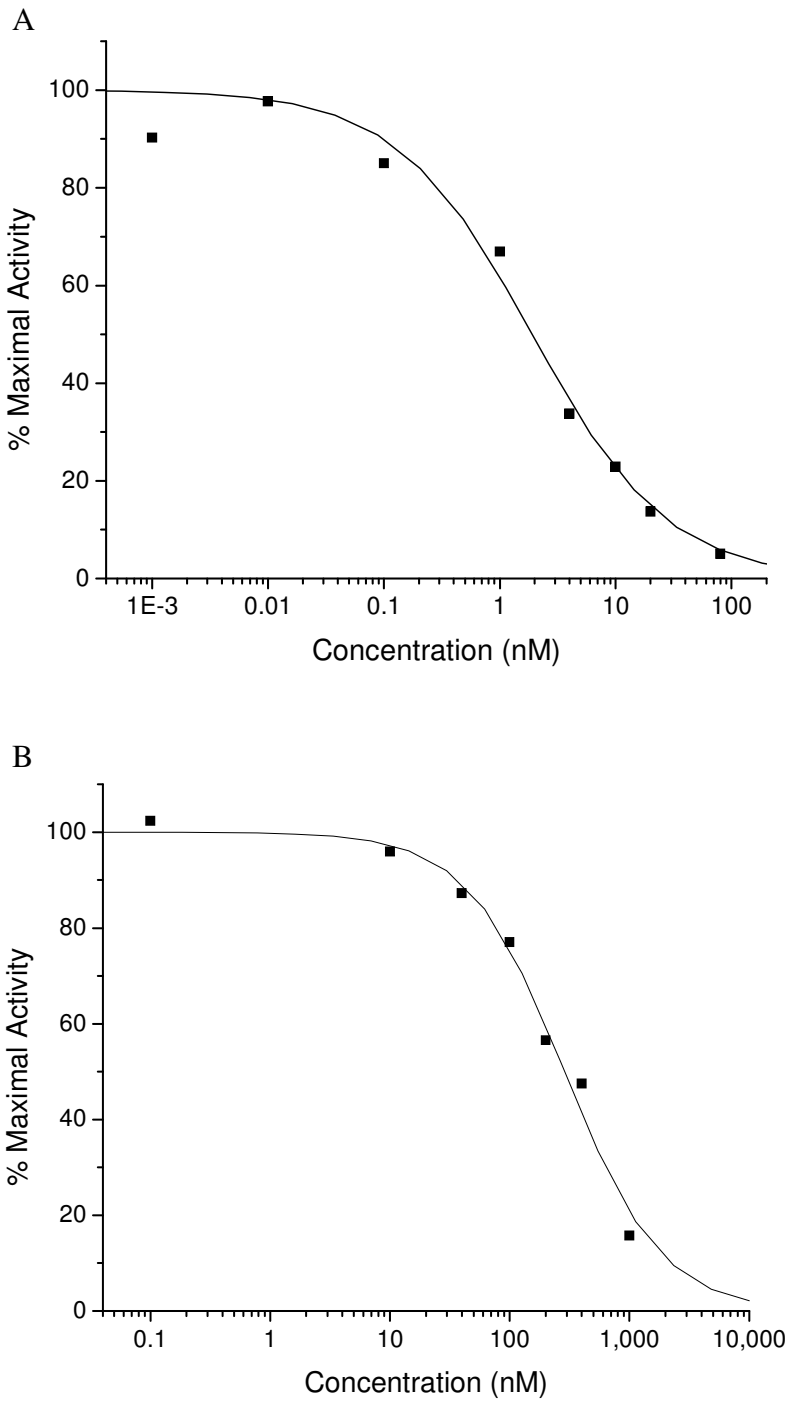

Figure SM25. Concentration-dependent inhibition of sACE-1 by (A) lisinopril and (B) fluorescein-lisinopril, from which IC_{50} values were obtained.

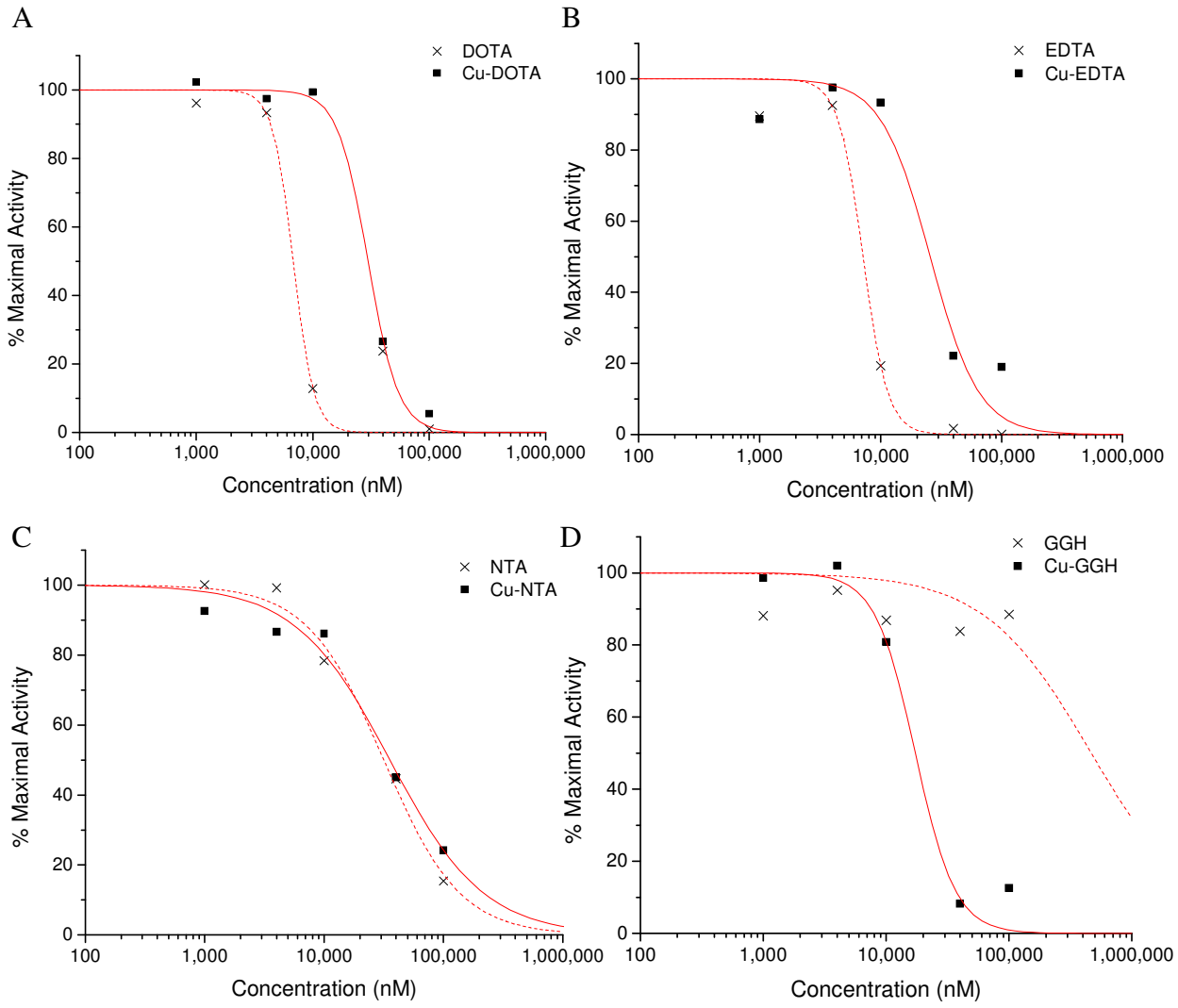

Figure SM26. Control experiments for concentration-dependent inhibition of sACE-1 by chelators and metal chelates lacking lisinopril. Metal chelates lacking lisinopril provided much weaker inhibition than the analogous metal-chelate-lisinopril complexes. Experiments were conducted in the same manner as for metal-chelate-lisinopril. (A) DOTA and Cu-DOTA; (B) EDTA and Cu-EDTA; (C) NTA and Cu-NTA; (D) GGH and Cu-GGH.

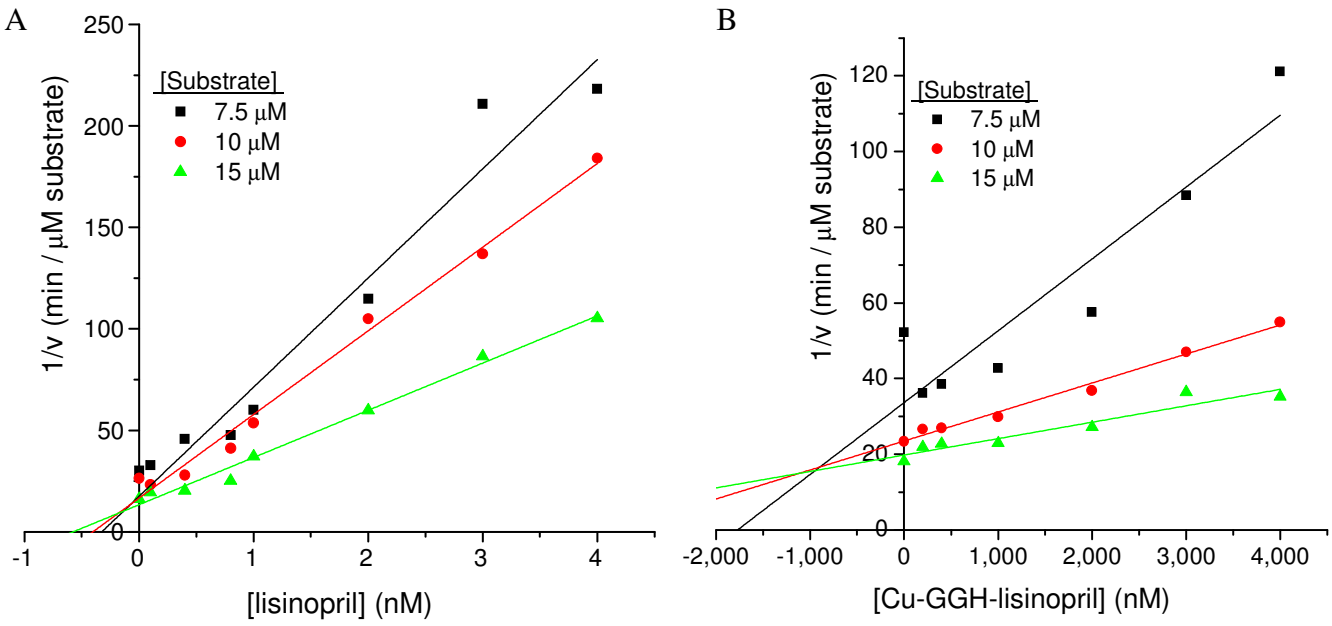

Figure SM27. Dixon plots for (A) lisinopril and (B) Cu-GGH-lisinopril support active site ACE binding and a competitive mode of inhibition for each inhibitor (lines intersect in upper-left quadrant). The concentration of ACE used was 1 nM, and the concentrations of the ACE substrate Abz-SDK(Dnp)P-OH used were 7.5 µM, 10 µM, and 15 µM. The resulting K_i values (~ 0.2 nM for lisinopril and ~ 900 nM for Cu-GGH-lisinopril) are consistent with the observed IC_{50} values.

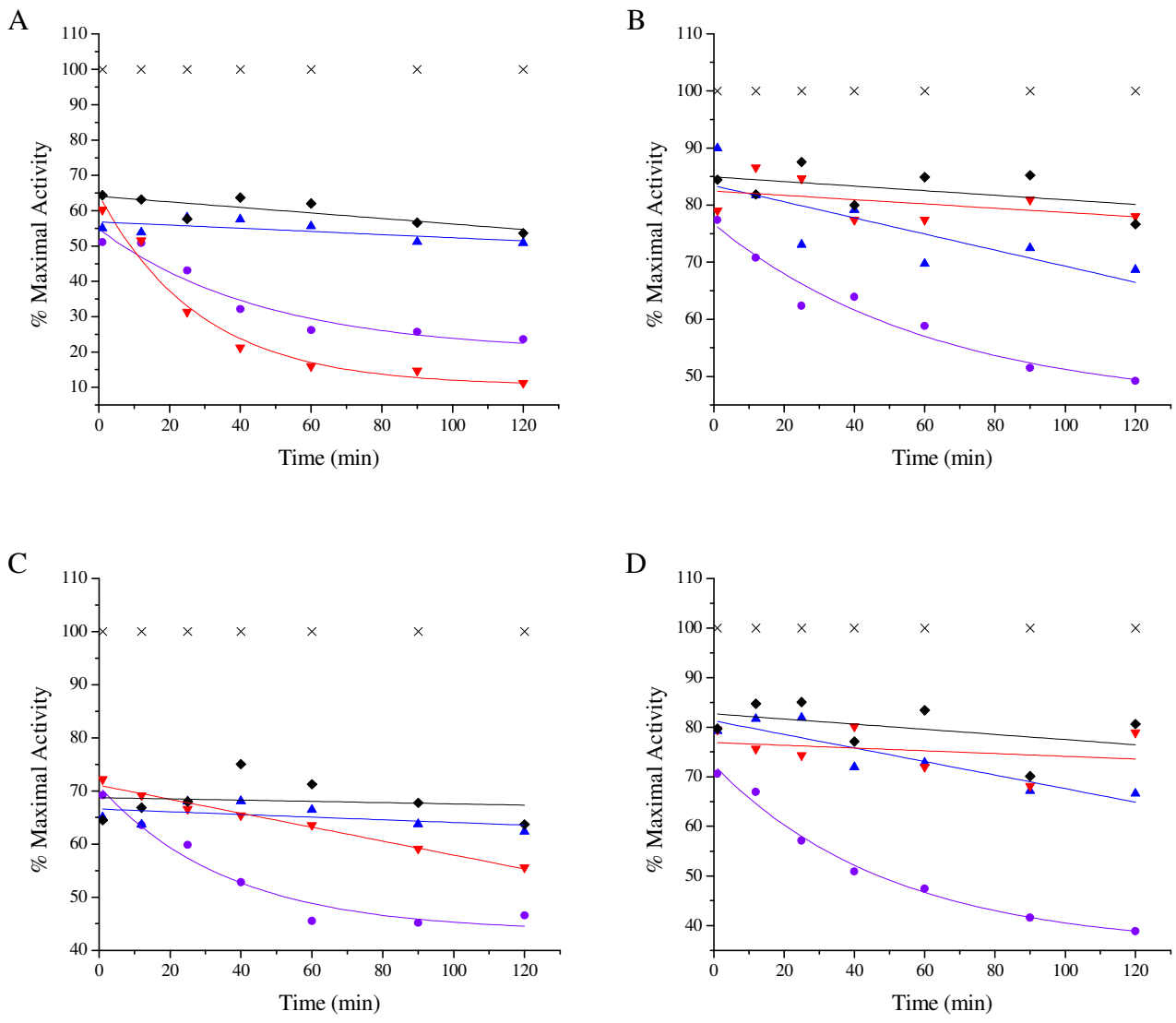

Figure SM28. Time-dependent inactivation of sACE-1 by (A) 865 nM Fe-DOTA-lisinopril, (B) 790 nM Co-DOTA-lisinopril, (C) 976 nM Ni-DOTA-lisinopril, and (D) 1,020 nM Cu-DOTA-lisinopril. sACE-1 (1 nM) was preincubated with metal-chelate-lisinopril complexes (at concentrations that initially allowed ≥ 60% sACE-1 activity) and also the coreactants 1 mM ascorbate and 1 mM H_2O_2 (●), 1 mM ascorbate (▲), 1 mM H_2O_2 (▼), or no coreactant (♦) for 2 hrs. At each time point within the preincubation period, an aliquot of the preincubation mixture was removed, mixed with fluorogenic substrate, and the fluorescence was monitored. At each time point, the initial rate of substrate cleavage (fluorescence intensity units per min) was quantified and expressed as a percentage of the rate of uninhibited substrate cleavage to give % maximal activity.

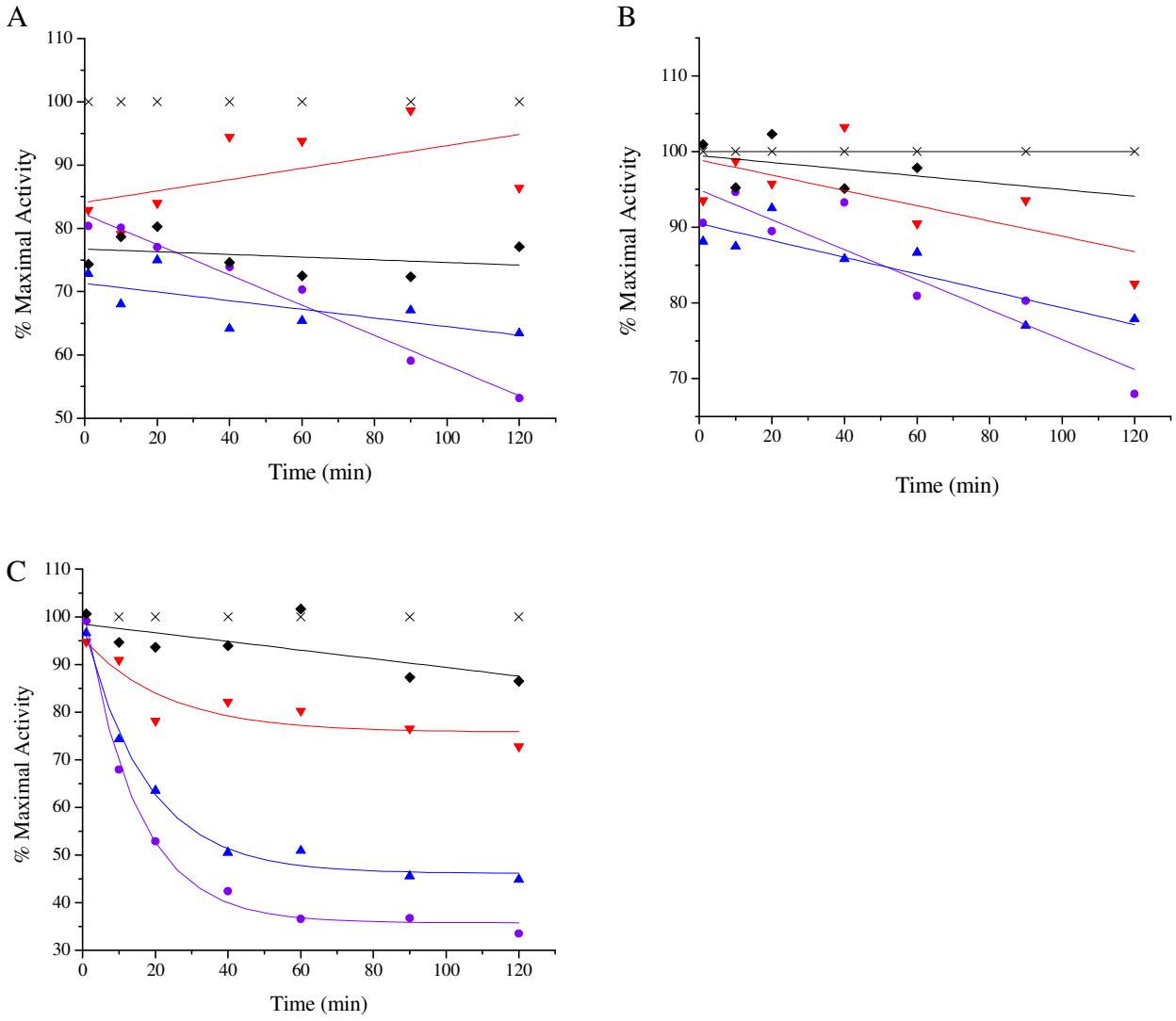

Figure SM29. Time-dependent inactivation of sACE-1 by (A) 19.7 nM Co-GGH-lisinopril, (B) 25 nM Ni-GGH-lisinopril, and (C) 300 nM Cu-GGH-lisinopril. sACE-1 (1 nM) was preincubated with metal-chelate-lisinopril complexes (at concentrations that initially allowed ≥ 60% sACE-1 activity) and also the coreactants 1 mM ascorbate and 1 mM H_2O_2 (●), 1 mM ascorbate (▲), 1 mM H_2O_2 (▼), or no coreactant (♦) for 2 hrs.

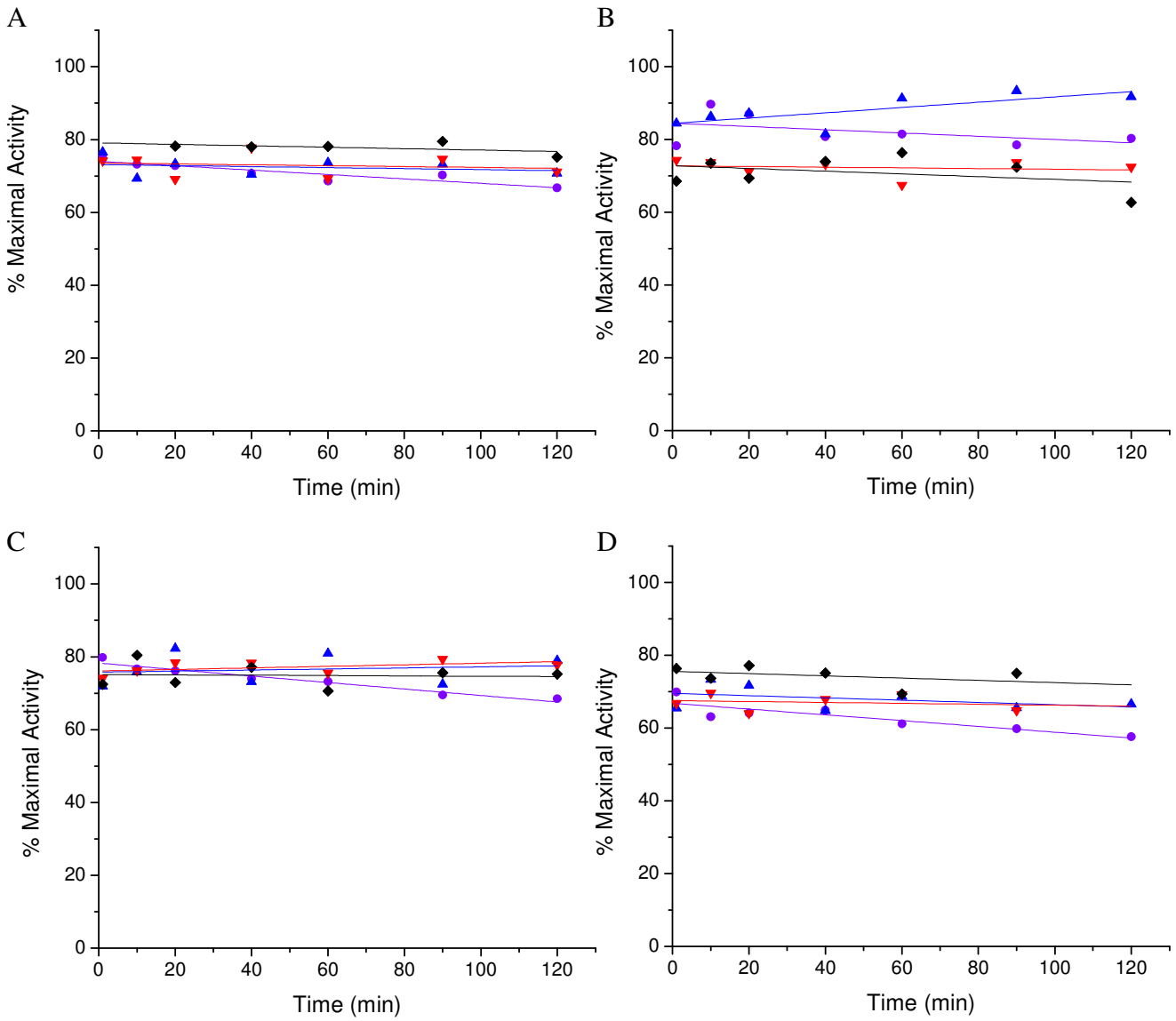

Figure SM30. Time-dependent inactivation of sACE-1 by (A) 7.8 nM Fe-NTA-lisinopril, (B) 4.8 nM Co-NTA-lisinopril, (C) 4.8 nM Ni-NTA-lisinopril, and (D) 14.4 nM Cu-NTA-lisinopril. sACE-1 (1 nM) was preincubated with metal-chelate-lisinopril complexes (at concentrations that initially allowed ≥ 60% sACE-1 activity) and also the coreactants 1 mM ascorbate and 1 mM H_2O_2 (●), 1 mM ascorbate (▲), 1 mM H_2O_2 (▼), or no coreactant (♦) for 2 hrs.

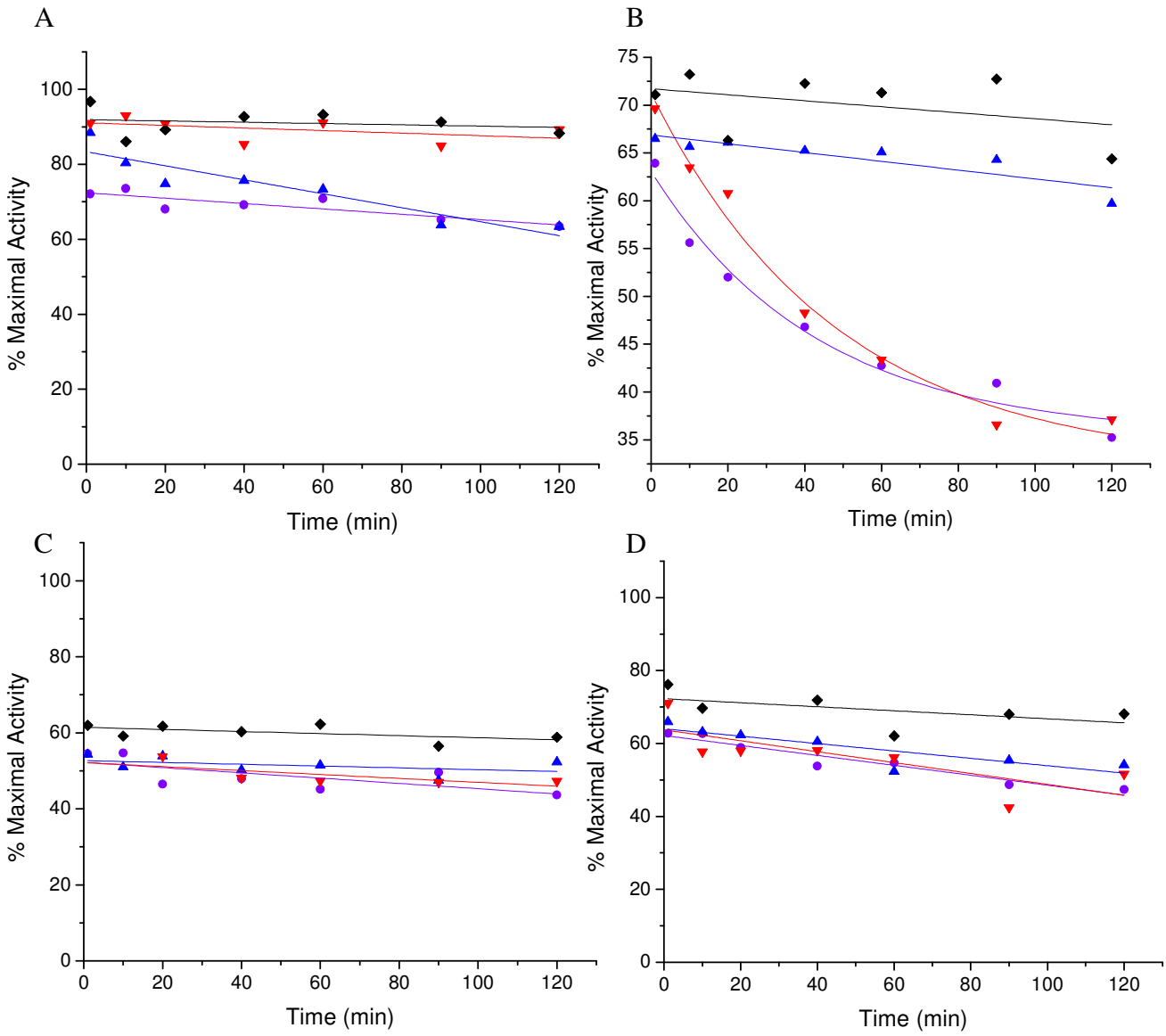

Figure SM31. Time-dependent inactivation of sACE-1 by (A) 14 nM Fe-EDTA-lisinopril, (B) 210 nM Co-EDTA-lisinopril, (C) 250 nM Ni-EDTA-lisinopril, and (D) 230 nM Cu-EDTA-lisinopril. sACE-1 (1 nM) was preincubated with metal-chelate-lisinopril complexes (at concentrations that initially allowed ≥ 60% sACE-1 activity) and also the coreactants 1 mM ascorbate and 1 mM H_2O_2 (●), 1 mM ascorbate (▲), 1 mM H_2O_2 (▼), or no coreactant (♦) for 2 hrs.

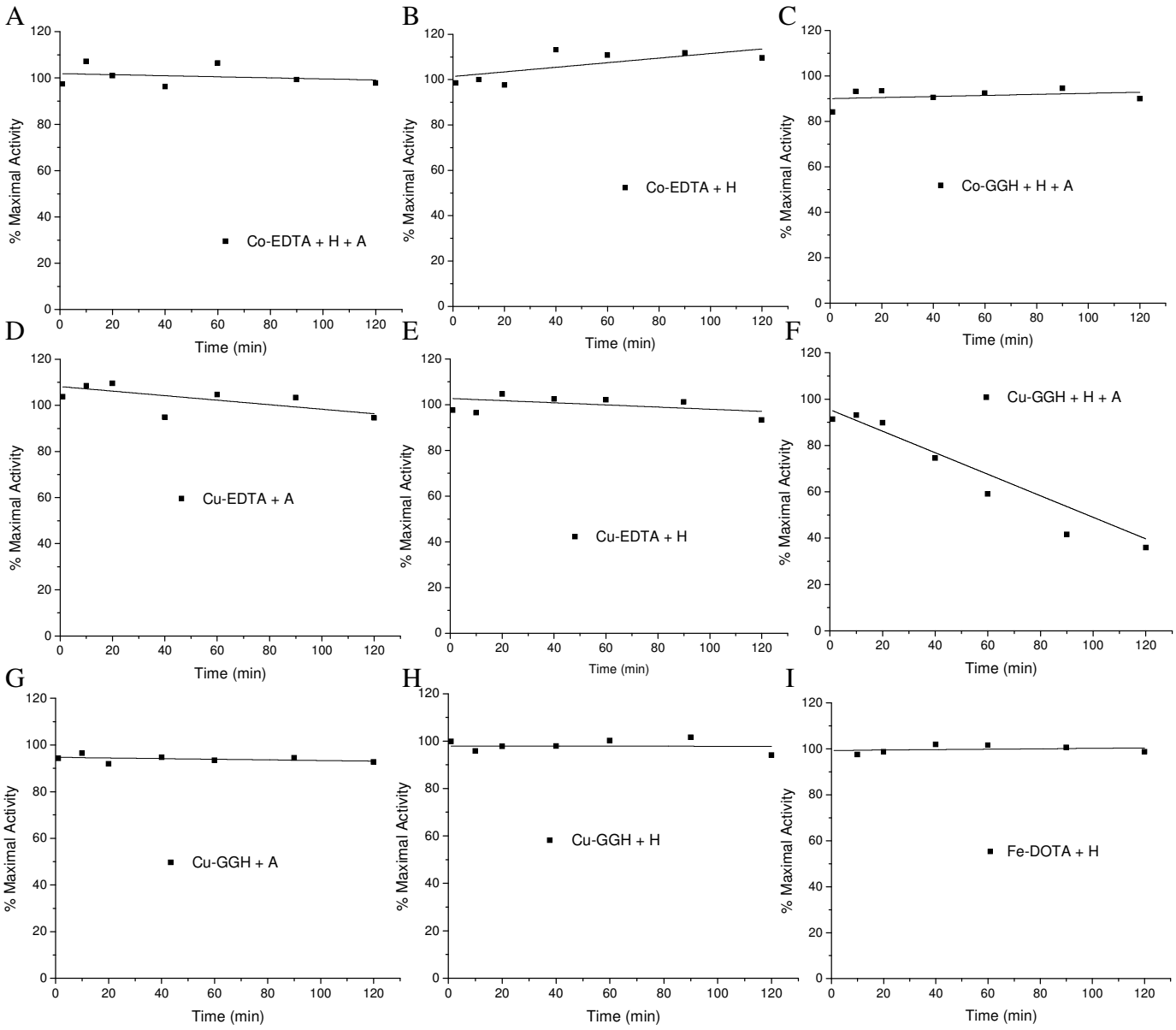

Figure SM32. Time-dependent inactivation of sACE-1 by M-chelates lacking attached lisinopril, using a variety of coreactant conditions (1 mM H_2O_2 and or ascorbate). (A) Co-EDTA with ascorbate and H_2O_2, (B) Co-EDTA with H_2O_2, (C) Co-GGH with ascorbate and H_2O_2, (D) Cu-EDTA with ascorbate, (E) Cu-EDTA with H_2O_2, (F) Cu-GGH with ascorbate and H_2O_2, (G) Cu-GGH with ascorbate, (H) Cu-GGH with H_2O_2, and (I) Fe-DOTA with H_2O_2. M-chelate/coreactant combinations were studied only for reactions for which the respective M-chelate-lisinopril complex provided an above-background rate of inactivation; the concentration of M-chelate used for time-dependent inactivation was the same as the concentration used for each M-chelate-lisinopril complex in the same assay.

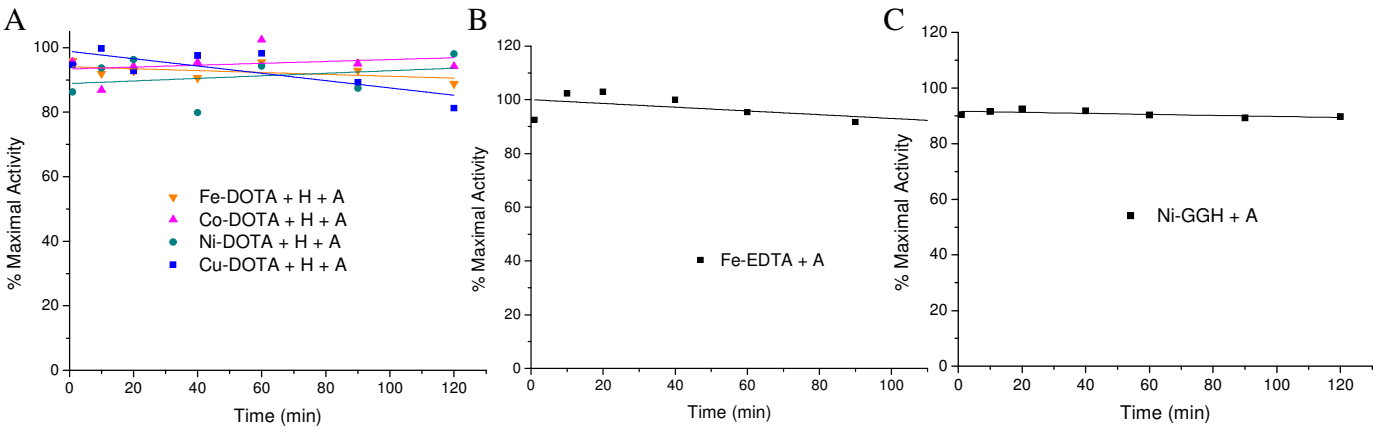

Figure SM32 (continued). Additional time-dependent inactivation of sACE-1 by M-chelates lacking attached lisinopril, using a variety of coreactant conditions (1 mM H_2O_2 and or ascorbate). (A) M-DOTA with ascorbate and H_2O_2, (B) Fe-EDTA with ascorbate, and (C) Ni-GGH with ascorbate. M-chelate/coreactant combinations were studied only for reactions for which the respective M-chelate-lisinopril complex provided an above-background rate of inactivation; the concentration of M-chelate used for time-dependent inactivation was the same as the concentration used for each M-chelate-lisinopril complex in the same assay.

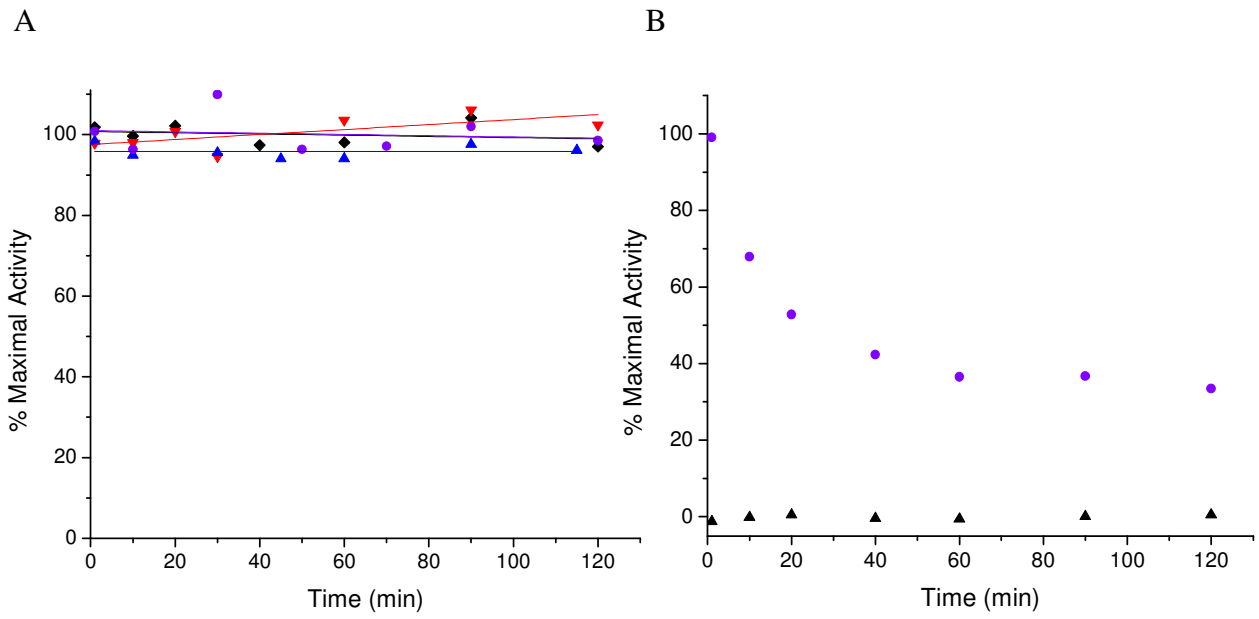

Figure SM33. Control experiments demonstrating (A) the absence of time-dependent inactivation of sACE-1 in the absence of catalyst, but with coreactants and (B) a lack of substrate cleavage with catalyst and coreactants but without sACE-1. (A) sACE-1 (1 nM) was preincubated with the coreactants 1 mM ascorbate and 1 mM H_2O_2 (●), 1 mM ascorbate (▲), 1 mM H_2O_2 (▼), or no coreactant (♦) for 2 hrs. (B) 300 nM Cu-GGH-lisinopril, 1 mM H_2O_2, and 1 mM ascorbate were preincubated for varied time intervals without sACE-1 (▲) and with 1 nM sACE-1 (●), and substrate cleavage activity at each time point was measured using the same method as described in the manuscript.

Complex	Second Order Rate Constant ($M^{-1}min^{-1}$) of sACE-1 Inactivation by M-chelate-lisinopril Complexes and Coreactants[a]			
	Ascorbate + H_2O_2	**Ascorbate**	**H_2O_2**	**None**
Fe-NTA-lisin	< 100,000	< 50,000	< 100,000	< 40,000
Co-NTA-lisin	< 200,000	< 90,000	< 200,000	< 100,000
Ni-NTA-lisin	< 200,000	< 100,000	< 200,000	< 80,000
Cu-NTA-lisin	< 60,000	< 30,000	< 60,000	< 30,000
Co-GGH-lisin	**70,000 ± 40,000**	20,000 ± 20,000	< 50,000	< 20,000
Ni-GGH-lisin	40,000 ± 40,000	**30,000 ± 20,000**	30,000 ± 40,000	< 30,000
Cu-GGH-lisin	**152,000 ± 7,000**	**102,000 ± 6,000**	**28,000 ± 9,000**	2,000 ± 2,000
Fe-EDTA-lisin	< 60,000	**110,000 ± 30,000**	< 60,000	< 30,000
Co-EDTA-lisin	**30,000 ± 10,000**	< 2,000	**40,000 ± 10,000**	< 2,000
Ni-EDTA-lisin	< 4,000	< 2,000	< 4,000	< 1,000
Cu-EDTA-lisin	2,000 ± 4,000	**3,000 ± 2,000**	**5,000 ± 4,000**	1,000 ± 2,000
Fe-DOTA-lisin	**8,000 ± 1,000**	100 ± 500	**22,000 ± 5,000**	< 900
Co-DOTA-lisin	**5,000 ± 1,000**	1,000 ± 1,000	< 1,000	< 500
Ni-DOTA-lisin	**7,000 ± 1,000**	< 400	1,100 ± 900	< 500
Cu-DOTA-lisin	**6,200 ± 900**	**1,000 ± 400**	< 900	200 ± 500

Table SM3. Summary of second order rate constants for inactivation of sACE-1 by metal-chelate-lisinopril complexes. Second order rate constants could not be precisely determined for many of the M-chelate-lisinopril complexes, especially those which required use of relatively low concentrations in time-dependent assays, due to excessive error propagation during conversion from initial rates to second order rate constants, and in such cases only an upper limit could be established. [a] Rate constants above background are shown in bold.

Complex	Initial Rate (% Activity / min)	Conditions
Cu-GGH	0.5 ± 0.1	Ascorbate + H_2O_2, pH 7.4, 37 ºC
Fe-EDTA	0.07 ± 0.07	Ascorbate, pH 7.4, 37 ºC
Cu-GGH	0.01 ± 0.02	Ascorbate, pH 7.4, 37 ºC
Co-GGH	< 0.03	Ascorbate + H_2O_2, pH 7.4, 37 ºC
Co-EDTA	< 0.06	H_2O_2, pH 7.4, 37 ºC
Co-EDTA	0.02 ± 0.04	Ascorbate + H_2O_2, pH 7.4, 37 ºC
Ni-GGH	0.01 ± 0.05	Ascorbate, pH 7.4, 37 ºC
Cu-GGH	< 0.03	H_2O_2, pH 7.4, 37 ºC
Fe-DOTA	< 0.02	H_2O_2, pH 7.4, 37 ºC
Fe-DOTA	0.03 ± 0.02	Ascorbate + H_2O_2, pH 7.4, 37 ºC
Ni-DOTA	< 0.06	Ascorbate + H_2O_2, pH 7.4, 37 ºC
Cu-DOTA	0.11 ± 0.04	Ascorbate + H_2O_2, pH 7.4, 37 ºC
Cu-EDTA	0.05 ± 0.04	H_2O_2, pH 7.4, 37 ºC
Co-DOTA	< 0.04	Ascorbate + H_2O_2, pH 7.4, 37 ºC
Cu-EDTA	0.1 ± 0.1	Ascorbate, pH 7.4, 37 ºC
Cu-DOTA	< 0.04	Ascorbate, pH 7.4, 37 ºC

Table SM4. Summary of control experiments for time-dependent inactivation of sACE-1 by metal-chelates lacking lisinopril. Control experiments were performed for M-chelate complexes and conditions for which above-background sACE-1 inactivation was observed with corresponding M-chelate-lisinopril complexes. The conditions used were the same as for time-dependent inactivation of sACE-1 by M-chelate-lisinopril complexes. These initial rates were used to obtain the second order rate constants for M-chelates listed in Table 4 of the manuscript.

A

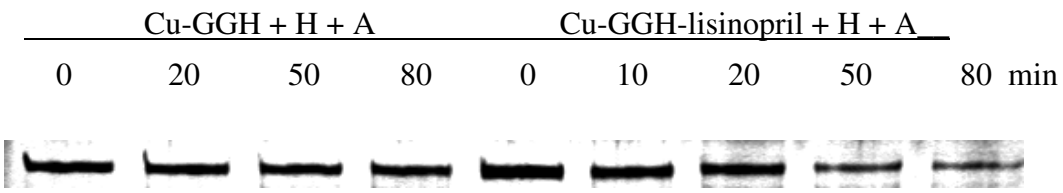

B

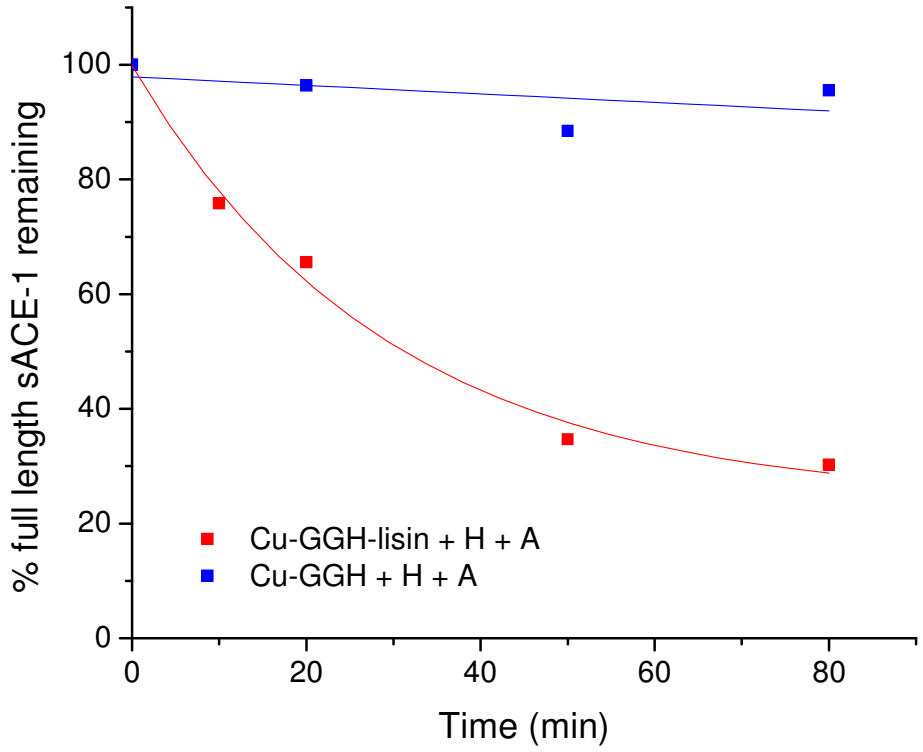

Figure SM34. Time-dependent cleavage of full length sACE-1 by Cu-GGH-lisinopril and Cu-GGH lacking attached lisinopril, with coreactants 1 mM ascorbate + 1 mM H_2O_2. For all time-dependent incubations, the concentration of M-chelate-lisin that gave 20% saturation of sACE-1 was used; the same concentrations were used for respective M-chelates lacking lisinopril. (A) Time-dependent cleavage was monitored by incubating sACE-1, catalysts, and coreactants for varied time intervals, followed by SDS-PAGE with silver staining. (B) Disappearance of full length sACE-1 over time was fit to a first order equation, and initial rates of cleavage (% sACE-1 / min) were determined. Cleavage of sACE-1, for which the rate was generally much slower than the rate of inactivation of sACE-1, was faster for M-chelate-lisinopril conjugates than for control complexes lacking lisinopril. Time-dependent cleavage was monitored for other reactions in the same manner.

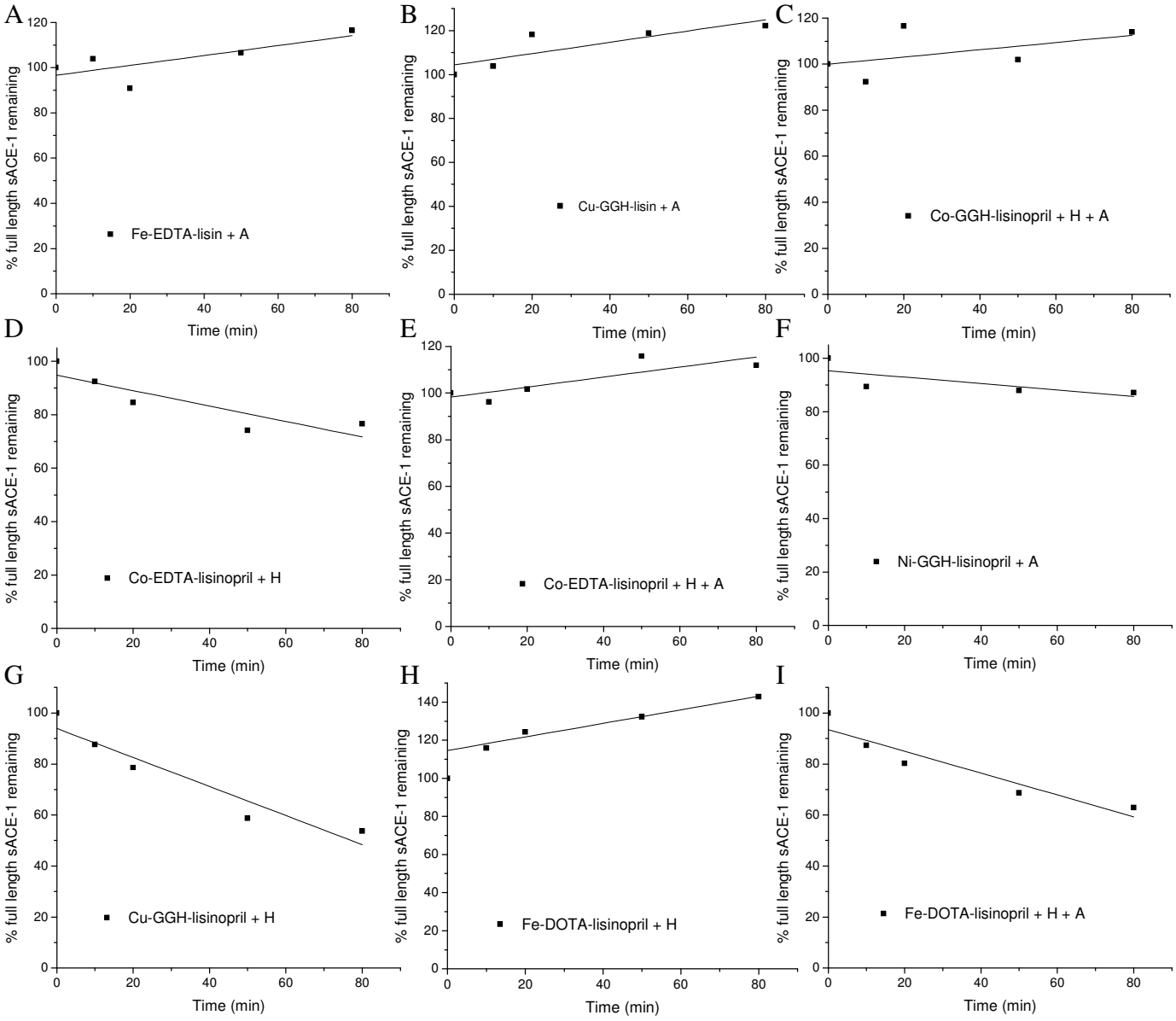

Figure SM34 (continued). Additional reactions of time-dependent cleavage of full length sACE-1 (monitored by SDS-PAGE with silver staining) by a variety of catalysts and coreactant conditions: (A) Fe-EDTA-lisinopril with ascorbate, (B) Cu-GGH-lisinopril with ascorbate, (C) Co-GGH-lisinopril with ascorbate and H_2O_2, (D) Co-EDTA-lisinopril with H_2O_2, (E) Co-EDTA-lisinopril with ascorbate and H_2O_2, (F) Ni-GGH-lisinopril with ascorbate, (G) Cu-GGH-lisinopril with H_2O_2, (H) Fe-DOTA-lisinopril with H_2O_2, and (I) Fe-DOTA-lisinopril with ascorbate and H_2O_2. Coreactants were present at 1 mM.

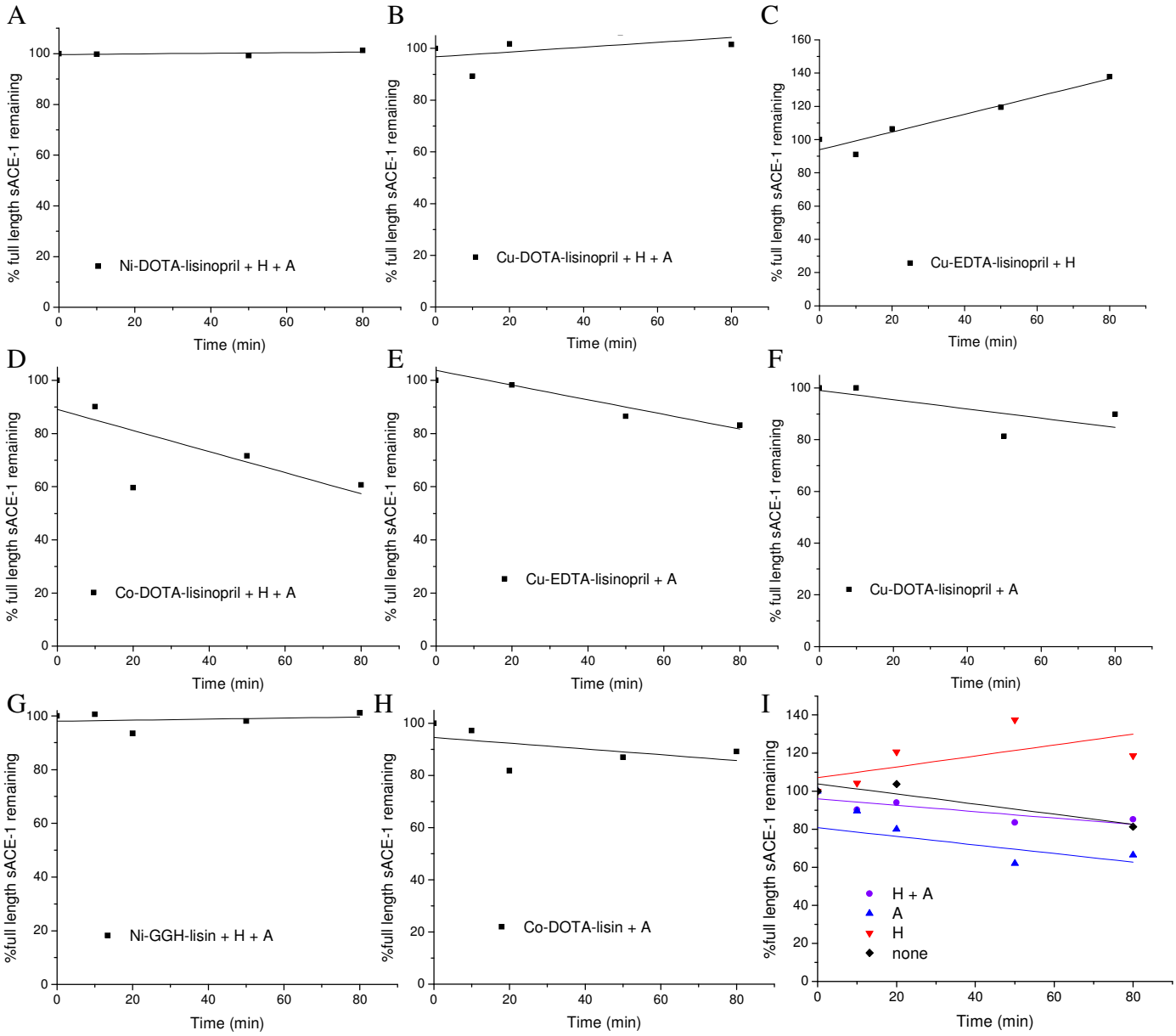

Figure SM34 (continued). Additional reactions of time-dependent cleavage of full length sACE-1 (monitored by SDS-PAGE with silver staining) by a variety of catalysts and coreactant conditions: (A) Ni-DOTA-lisinopril with ascorbate and H_2O_2, (B) Cu-DOTA-lisinopril with ascorbate and H_2O_2, (C) Cu-EDTA-lisinopril with H_2O_2, (D) Co-DOTA-lisinopril with ascorbate and H_2O_2, (E) Cu-EDTA-lisinopril with ascorbate, (F) Cu-DOTA-lisinopril with ascorbate, (G) Ni-GGH-lisinopril with ascorbate and H_2O_2, (H) Co-DOTA-lisinopril with ascorbate, and (I) control reactions containing various combinations of coreactants but no metal complex. Coreactants were present at 1 mM.

Reaction	Initial Rate (% sACE-1 / min)	First Order Rate Constant (min^{-1})	Second Order Rate Constant ($M^{-1}min^{-1}$)
Cu-GGH-lisin + H + A	2.6 ± 0.6	.026 ± 0.006	70,000 ± 20,000
Cu-GGH + H + A	0.07 ± 0.08	0.0007 ± 0.0008	< 3,000
Cu-GGH-lisin + H	0.6 ± 0.1	0.006 ± 0.001	15,000 ± 6,000
Co-GGH-lisin + H + A	< 0.2	< 0.002	< 70,000
Ni-GGH-lisin + A	0.12 ± 0.08	0.0012 ± 0.0008	< 60,000
Fe-DOTA-lisin + H	< 0.04	< 0.0004	< 2,000
Fe-DOTA-lisin + H + A	0.43 ± 0.08	0.0043 ± 0.0008	3,000 ± 1,000
Cu-DOTA-lisin + H + A	< 0.1	< 0.001	< 1,000
Cu-DOTA-lisin + A	0.2 ± 0.1	0.002 ± 0.001	< 2,000
Co-EDTA-lisin + H + A	< 0.08	< 0.0008	< 3,000
Co-EDTA-lisin + H	0.29 ± 0.09	0.0029 ± 0.0009	10,000 ± 7,000
Cu-EDTA-lisin + H	< 0.09	< 0.0009	< 9,000
Cu-EDTA-lisin + A	0.28 ± 0.07	0.0028 ± 0.0007	2,000 ± 9,000
Ni-DOTA-lisin + H + A	< 0.01	< 0.0001	< 600
Co-DOTA-lisin + H + A	0.4 ± 0.2	0.004 ± 0.002	2,000 ± 2,000
Fe-EDTA-lisin + A	< 0.1	< 0.001	< 100,000
Fe-EDTA + A	0.3 ± 0.2	< 0.006	< 100,000
Cu-GGH-lisin + A	< 0.09	< 0.0009	< 6,000
Ni-GGH-lisin + H + A	< 0.05	< 0.0005	< 20,000
Co-DOTA-lisin + A	0.1 ± 0.1	0.001 ± 0.001	< 2,000
Ni-DOTA-lisin + H	< 0.1	< 0.001	< 2,000
H + A	0.17 ± 0.07	0.0017 ± 0.0007	
A	0.2 ± 0.2	0.002 ± 0.002	
H	< 0.2	< 0.002	
None	< 0.4	< 0.004	

Table SM5. Summary of the initial rates, first order rate constants, and second order rate constants for all time-dependent sACE-1 cleavage reactions, monitored by SDS-PAGE with silver staining. Time-dependent cleavage reactions were only studied for catalysts/conditions that gave above background rates of time-dependent inactivation of sACE-1, since cleavage of full length sACE-1 is not expected if the enzyme remains active. Background rates of cleavage in the absence of catalyst, but with coreactants, were also determined. Coreactants were present at 1 mM; M-chelate-lisinopril complexes were present at the concentration that gave 20% saturation of 20 nM sACE-1, and M-chelates were present at the same concentration as the respective M-chelate-lisinopril complexes.

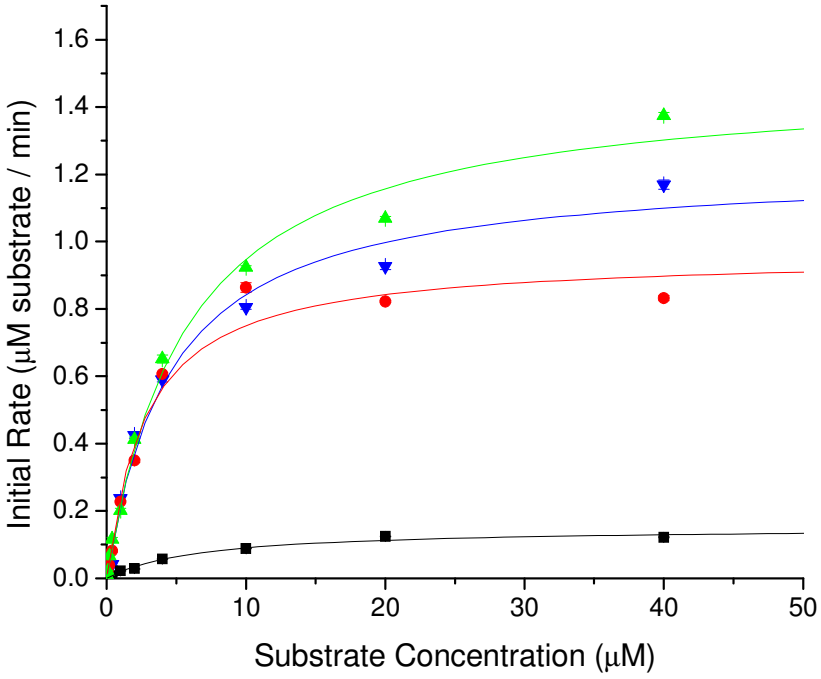

sACE-1 Preincubation Conditions	**k_{cat} (min^{-1})**	**K_M (μM)**	**k_{cat}/K_M ($min^{-1}μM^{-1}$)**
Cu-GGH-lisin + H_2O_2 + ascorbate, 15 h, 37 ºC	150 ± 10	7 ± 1	22 ± 4
Cu-GGH-lisin, 15 h, 37 ºC (control)	960 ± 50	2.8 ± 0.5	340 ± 70
H_2O_2 + ascorbate, 15 h, 37 ºC (control)	1,220 ± 50	4.5 ± 0.6	270 ± 40
None (control)	1,490 ± 60	5.7 ± 0.7	260 ± 30

Figure SM35. Michaelis-Menten kinetics of substrate cleavage by inactivated sACE-1. sACE-1 was inactivated by preincubation with 300 nM Cu-GGH-lisinopril, 1 mM H_2O_2, and 1 mM ascorbate for 15 h at 37 ºC (■, black). Following preincubation, sACE-1 was mixed with variable concentration of fluorogenic substrate, and substrate cleavage was monitored by fluorimetry. A control preincubation was performed with sACE-1 and Cu-GGH-lisinopril but without the coreactants H_2O_2 and ascorbate (●, red). Another control preincubation was performed with sACE-1 and coreactants but without catalyst (▼, blue). Another control was performed without preincubation of sACE-1 (▲, green). Two major effects were observed for catalytic inactivation of sACE-1 by Cu-GGH-lisinopril with coreactants: diminished substrate binding affinity for inactivated sACE-1 (higher K_M) and diminished catalysis of cleavage of enzyme-bound substrate by inactivated sACE-1 (lower k_{cat}). Inactivated sACE-1 thus retained some residual activity, although the enzyme efficiency (k_{cat}/K_M) of inactivated sACE-1 was significantly reduced (~ 12-fold reduction).

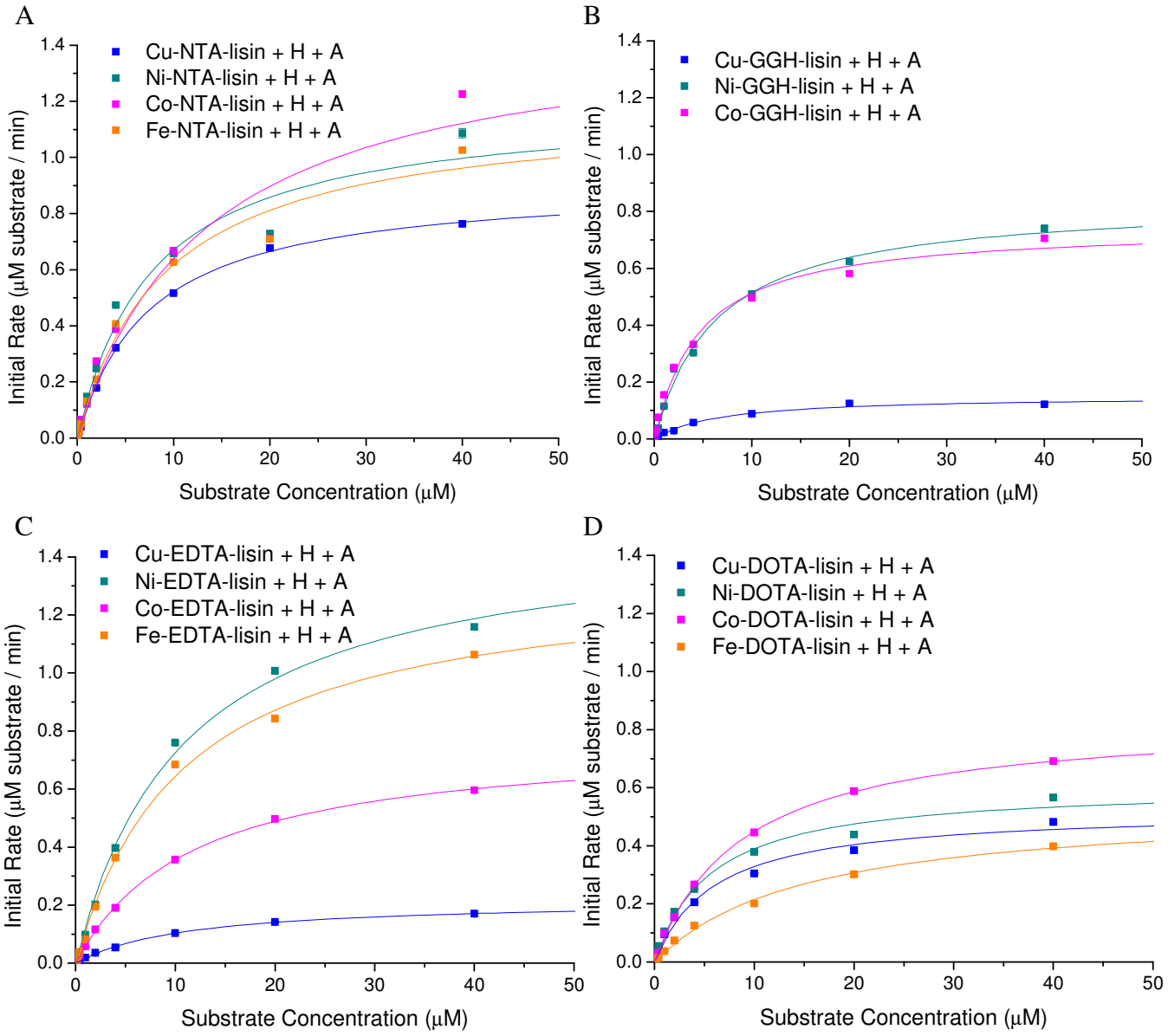

Figure SM36. Michaelis-Menten kinetics of substrate cleavage by inactivated sACE-1, after preincubation with (A) M-NTA-lisinopril, (B) M-GGH-lisinopril, (C) M-EDTA-lisinopril, and (D) M-DOTA-lisinopril and coreactants peroxide (H) and ascorbate (A). Plots of initial rate vs substrate concentration were fit to the Michaelis-Menten equation, and the resulting k_{cat}, K_M, and k_{cat}/K_M values are listed in the manuscript.

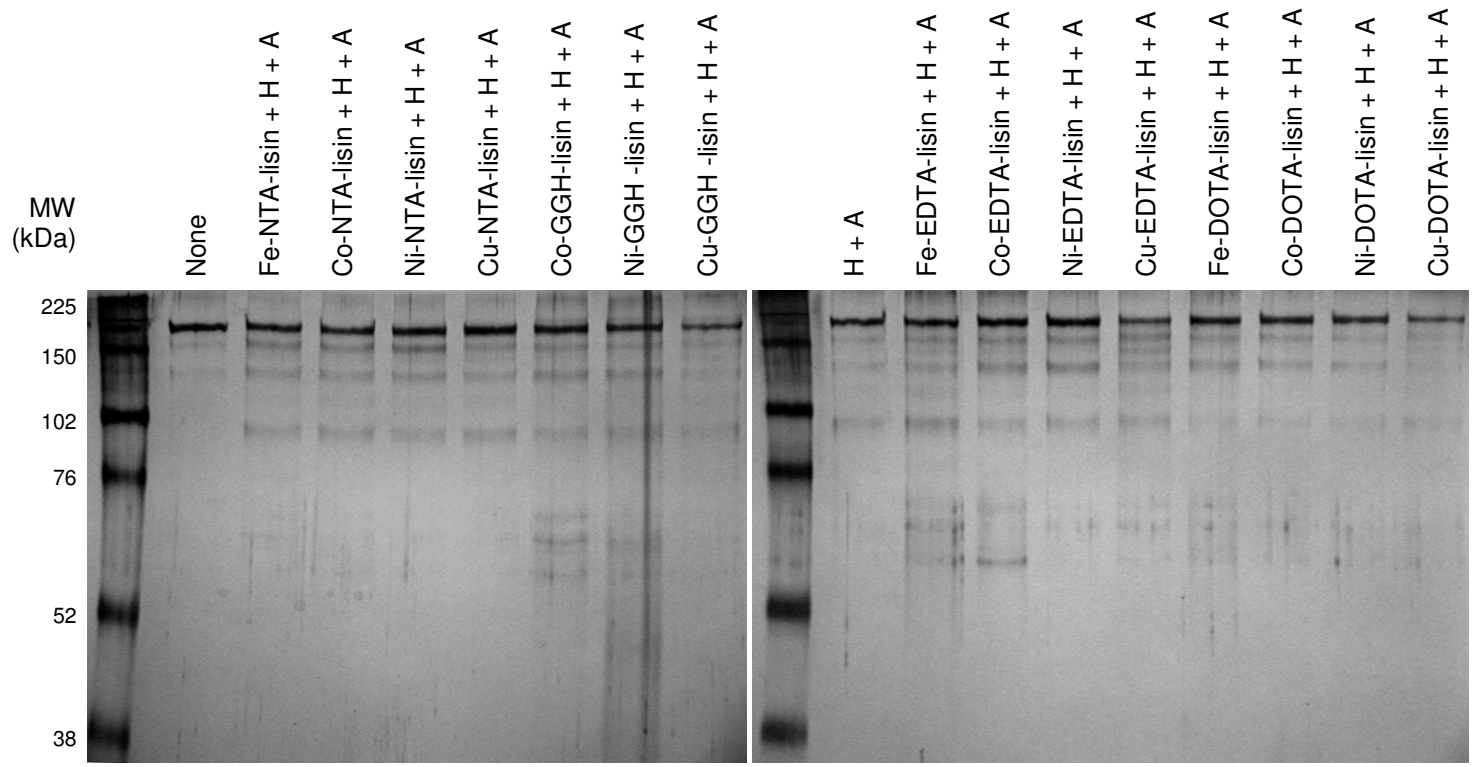

Figure SM37. Cleavage of sACE-1 by each M-chelate-lisinopril complex with co-reactants H_2O_2 (H) and ascorbate (A). Each reaction contained 20 nM sACE-1 (~ 50 ng), 1 mM H_2O_2, 1 mM ascorbate, and the concentration of M-chelate-lisinopril that gave 20% inhibition of sACE-1. Reactions were incubated for 15 h at 37 ºC. Following reaction, the reaction mixtures were mixed with loading buffer (denaturing/reducing conditions), boiled for 20 min, and separated by 7.5% SDS-PAGE, with silver staining to visualize sACE-1 and cleavage products. Reaction conditions were similar to the preincubation conditions used for Michaelis-Menten characterization of inactivated ACE. MW marker sizes are listed on the left side. To quantify sACE-1 and cleavage products within each lane, the intensity of each band was quantified, converted to moles using the apparent molecular weight (cubic spline calibration curve from MW marker), and then the % full length sACE-1 remaining (mol %) was determined following each reaction. The % full length sACE-1 remaining, relative to the control lacking complex but including coreactants, are listed in the manuscript for each reaction.

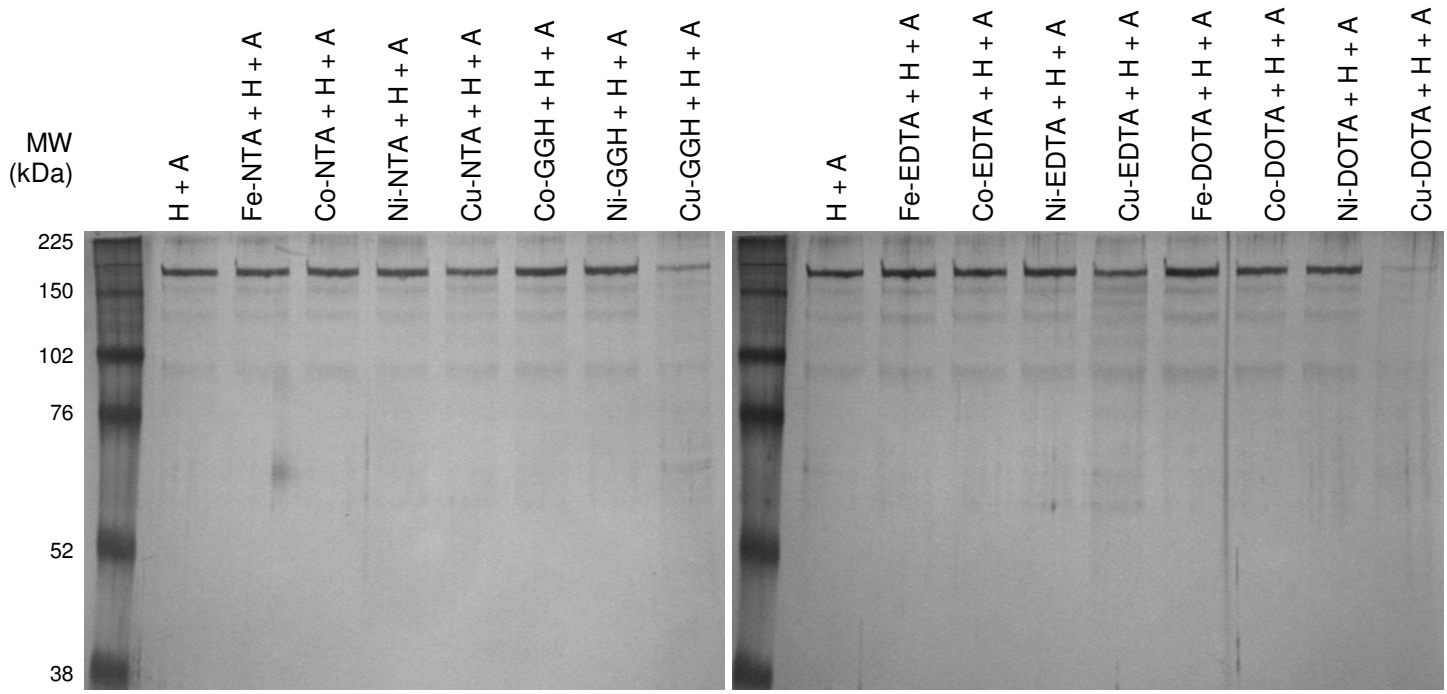

Figure SM38. Cleavage of sACE-1 by each M-chelate lacking attached lisinopril with co-reactants H_2O_2 (H) and ascorbate (A). Each reaction contained 20 nM sACE-1 (~ 50 ng), 1 mM H_2O_2, 1 mM ascorbate, and conditions were similar to the preincubation conditions used for Michaelis-Menten characterization of inactivated ACE. Reactions were run for 15 h at 37 ºC, and conditions were the same as for M-chelate-lisinopril complexes. The cleavage products formed after incubation with M-chelates lacking attached lisinopril were similar in size to the bands observed for M-chelate-lisinopril complexes, although cleavage appeared to occur at a slower rate for M-chelates than for M-chelate-lisinopril complexes (see data for time-dependent cleavage of sACE-1, in this supporting information).

Complex / Coreactants	% full length sACE-1 remaining after 15 h incubation	
	M-chelate-lisinopril	M-chelate without lisinopril
Fe-NTA-lis + H + A	70 ± 20	~90
Co-NTA-lis + H + A	70 ± 20	~70
Ni-NTA-lis + H + A	70 ± 10	~70
Cu-NTA-lis + H + A	72 ± 2	~60
Co-GGH-lis + H + A	60 ± 30	~80
Ni-GGH-lis + H + A	60 ± 30	~70
Cu-GGH-lis + H + A	40 ± 20	~30
Fe-EDTA-lis + H + A	60 ± 30	~70
Co-EDTA-lis + H + A	60 ± 30	~70
Ni-EDTA-lis + H + A	70 ± 10	~60
Cu-EDTA-lis + H + A	30 ± 20	~40
Fe-DOTA-lis + H + A	70 ± 10	~70
Co-DOTA-lis + H + A	70 ± 10	~60
Ni-DOTA-lis + H + A	70 ± 10	~70
Cu-DOTA-lis + H + A	60 ± 10	~20
Free Fe + H + A	~80	
Free Co + H + A	~90	
Free Ni + H + A	~90	
Free Cu + H + A	~30	
Free Fe	~90	
Free Co	~100	
Free Ni	~90	
Free Cu	~90	
Cu-GGH-lis + H + A	40 ± 10	
Cu-GGH-lis + H	60 ± 10	
Cu-GGH-lis + A	60 ± 8	
Cu-GGH-lis	90 ± 20	
sACE-1 + H + A	70 ± 6	
sACE-1 + H	80 ± 20	
sACE-1 + A	90 ± 20	
sACE-1	100 ± 10	

Table SM6. Summary of all data for % full length sACE-1 remaining after 15 h preincubations with catalysts (that gave 20% saturation of sACE-1) with and without attached lisinopril (all with 1 mM H_2O_2 and 1 mM ascorbate), free metal ions (100 nM each) with and without H_2O_2 and ascorbate (1 mM each when present), and other control reactions with varied combinations of coreactants (each 1 mM when present). The % remaining sACE-1 where calculated as described in the manuscript. The data listed in the manuscript for the 15 h reactions are listed as % sACE-1 remaining relative to the % sACE-1 remaining in the relevant control reaction containing H_2O_2 and ascorbate, which was adjusted to 100%.

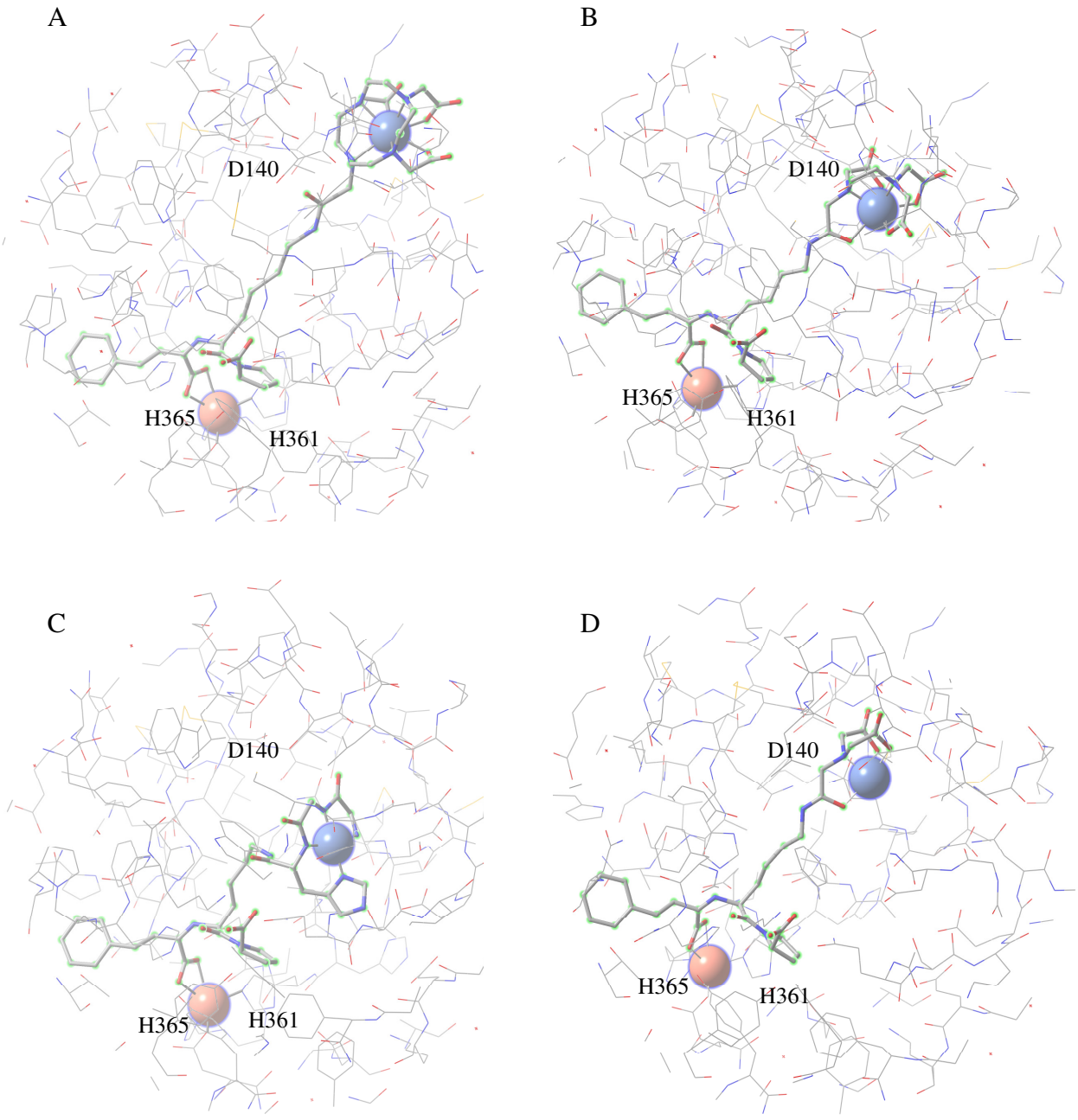

Figure SM39. Energy-minimized structural models of ACE (N-domain) active site binding by (A) Fe-DOTA-lisinopril, (B) Fe-EDTA-lisinopril, (C) Cu-GGH-lisinopril, and (D) Fe-NTA-lisinopril. The redox-active metal for each M-chelate-lisinopril complex is shown as a blue sphere (upper right within each model), and the active site Zn^{2+} is shown as a pink sphere (bottom left within each model). Residue D140 can interact with the lysine sidechain of unmodified lisinopril, while H361 and H365 form part of the conserved HEXXH Zn^{2+}-binding motif.

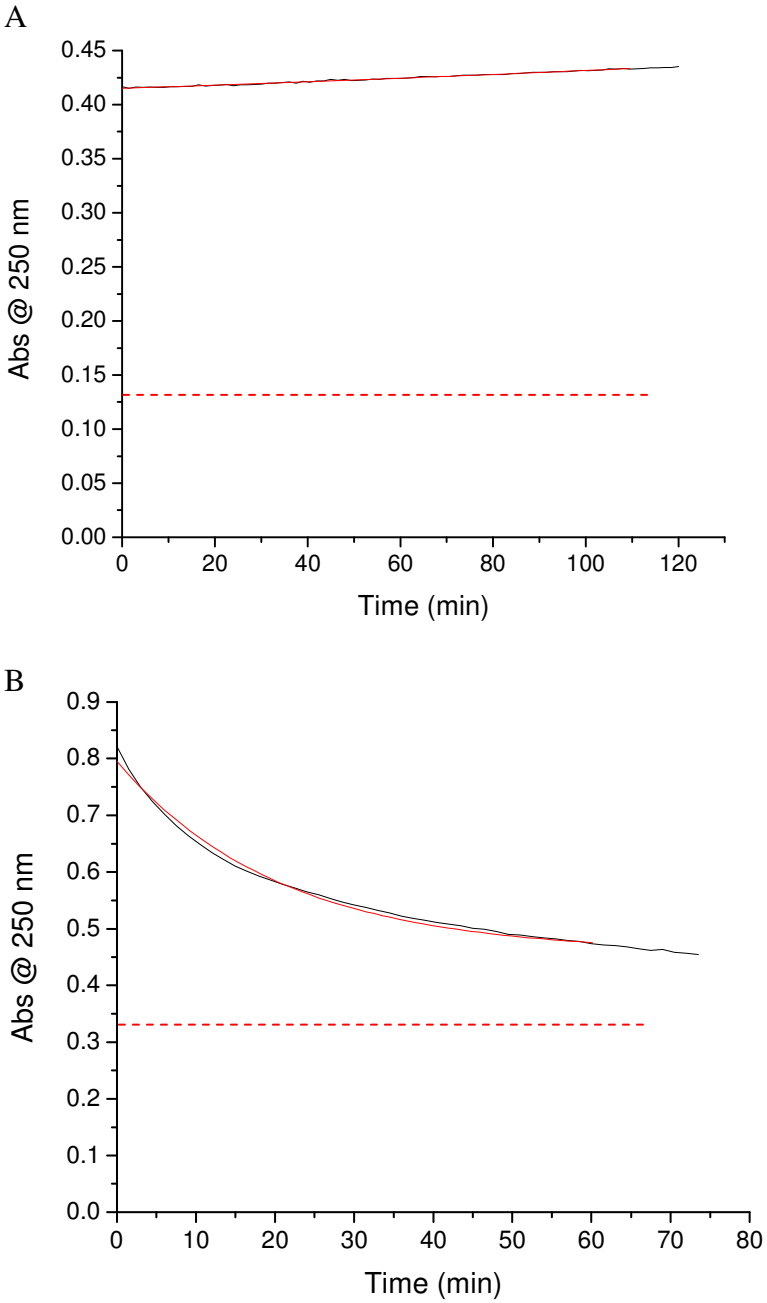

Figure SM40. Metal displacement from 100 µM metal chelates in the presence of 100 µM Zn^{2+} monitored by UV/Vis spectroscopy. (A) Cu-GGH was stable in the presence of Zn^{2+}. (B) Fe was displaced from Fe-EDTA by Zn^{2+} with a rate constant of 350 ± 10 $M^{-1}min^{-1}$. Calculated absorbance of free metals are indicated by the dashed lines (Abs = 0.13 for 100 µM free Cu at 250 nm; Abs = 0.33 for 100 µM free Fe at 250 nm). Experiments were repeated, and initial rates and second order rate constants for metal displacement by Zn^{2+} were calculated, for all metal chelates.

Rate of Metal Displacement (μM/min) from M-chelates with 100 μM M-chelate and 100 μM $ZnCl_2$				
	Fe^{3+}	Co^{2+}	Ni^{2+}	Cu^{2+}
DOTA	0.031 ± 0.001	< 0.003	< 0.003	< 0.004
EDTA	3.5 ± 0.1	4.8 ± 0.2	< 0.05	< 0.004
NTA	< 0.0003	< 0.07	< 0.1	< 0.02
GGH		< 0.03	< 0.0004	< 0.02
Second Order Rate Constant for Metal Displacement from M-chelates ($M^{-1}min^{-1}$) by Zn^{2+}				
	Fe^{3+}	Co^{2+}	Ni^{2+}	Cu^{2+}
DOTA	3.1 ± 0.1	< 0.3	< 0.3	< 0.4
EDTA	350 ± 10	480 ± 20	< 5	< 0.4
NTA	< 0.03	< 7	< 10	< 2
GGH		< 3	< 0.04	< 2

Table SM7. Summary of observed initial rates and second order rate constants for metal displacement from 100 μM metal chelates in the presence of 100 μM Zn^{2+} monitored by UV/Vis spectroscopy. All complexes were effectively stable in the presence of Zn^{2+}, except for Fe-EDTA, Co-EDTA, and Fe-DOTA, at concentrations of 100 μM Zn^{2+}. Second order rate constants were calculated from initial rates based on the following equation: Rate = k_2.[M-chelate].[Zn^{2+}]. The concentrations of Zn^{2+} (10 μM) and metal-chelate-lisinopril complexes (1 nM – 100 μM) used for the concentration-dependent and time-dependent inactivation of sACE-1 by metal-chelate-lisinopril complexes were generally far lower than those used here, and rates of metal displacement by Zn^{2+} for all species are likely to be insignificant in the sACE-1 inactivation assays. For example, Fe displacement from Fe-EDTA by Zn^{2+} has a second order rate constant of 350 ± 10 $M^{-1}min^{-1}$, and at 10 μM Zn^{2+} and 1 μM Fe-EDTA, Fe would be lost at a calculated rate of only ~ 3.5×10^{-9} M/min, or 0.35 % of the metal complex per minute.

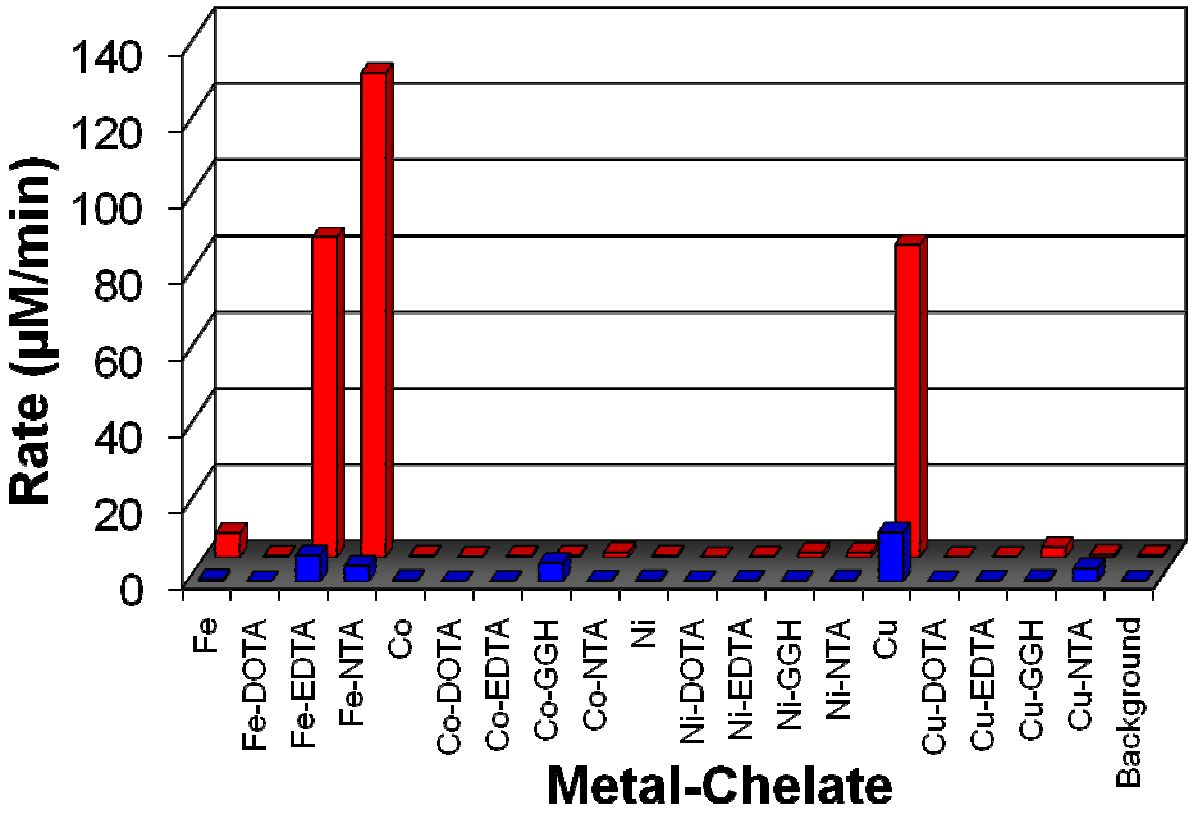

Figure SM41. Summary of initial rates for multiple turnover consumption of ascorbate by a variety of M-chelates. Rates are shown for each M-chelate/O_2 (front) and M-chelate/H_2O_2 (rear) combination. These data allow an independent assessment of the relative rate at which ascorbate might be consumed in the reactions of M-chelate-lisinopril/coreactants/sACE-1, using the same M-chelates and coreactants, under similar conditions. The concentrations were 1 mM ascorbate, 10 µM M-chelate, 1 mM H_2O_2 (when present). Reactions were performed in a buffer containing 20 mM HEPES, 100 mM NaCl, pH 7.4 at room temperature. Joyner et al. (2011).[8]

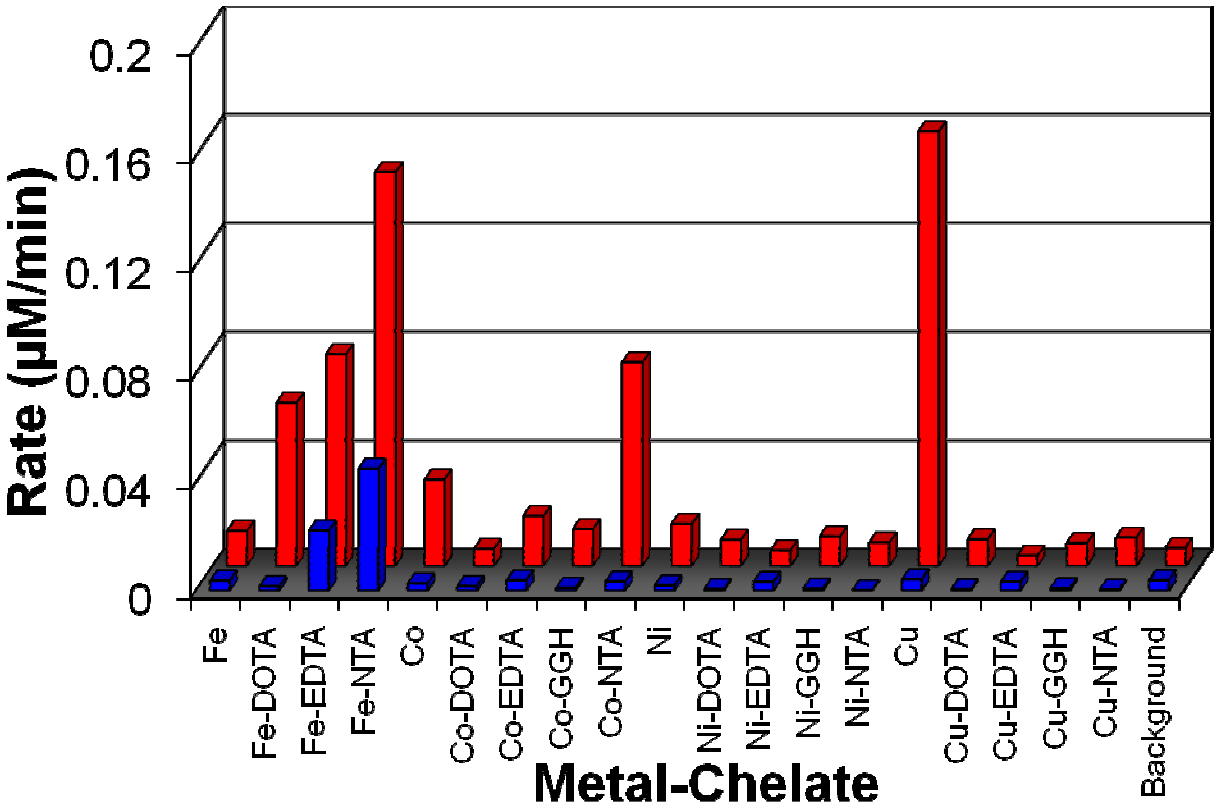

Figure SM42. Summary of steady-state rates of radical generation for a variety of M-chelates, monitored by TEMPO-9-AC fluorescence over time. Rates are shown for M-chelate/O_2 (front) and M-chelate/H_2O_2 (rear) combinations. These data allow an independent assessment of the relative rate at which diffusible superoxide and/or hydroxyl radicals might be generated in the reactions of M-chelate-lisinopril/coreactants/sACE-1, using the same M-chelates and coreactants, under similar conditions. The initial concentrations were 10 µM M-chelate, 10 µM TEMPO-9-AC, 1 mM H_2O_2 (when present). Reactions were performed in a buffer containing 20 mM HEPES, 100 mM NaCl, pH 7.4 at room temperature. Joyner et al. (2011).[8]

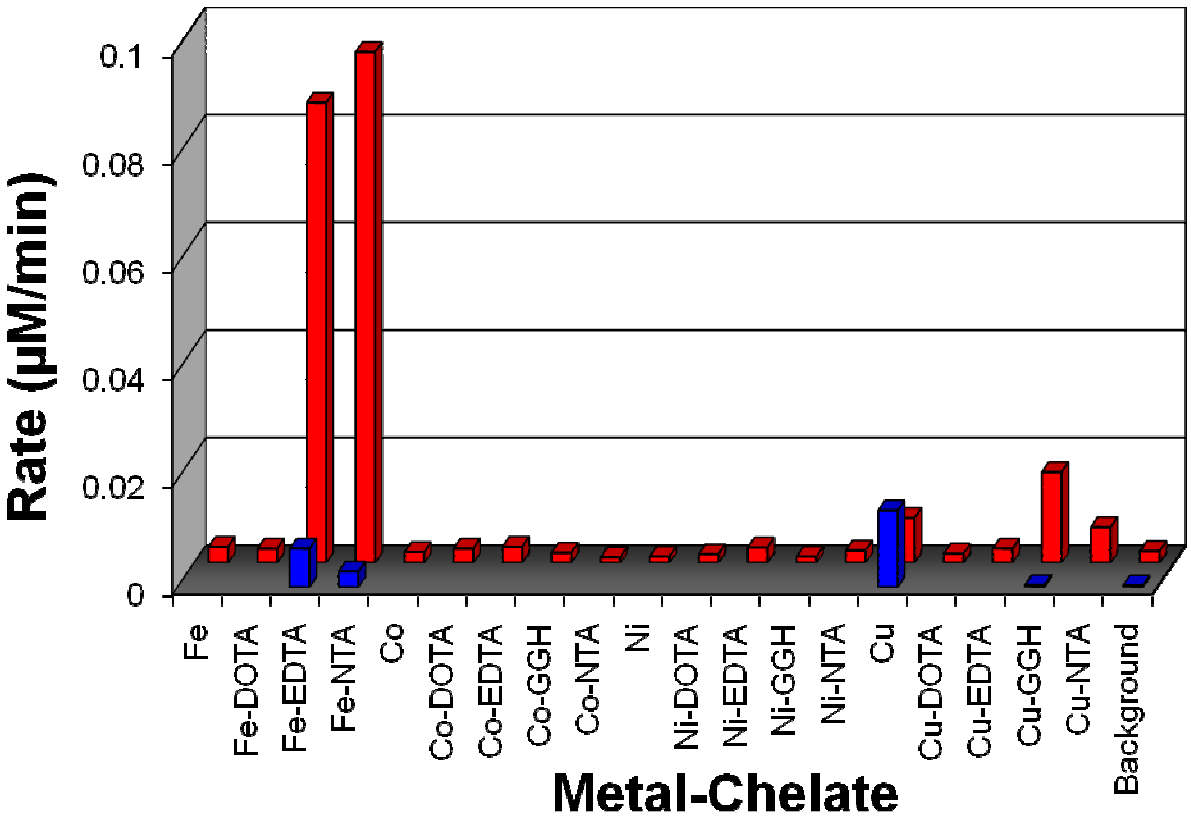

Figure SM43. Summary of steady-state rates of hydroxyl radical generation for a variety of M-chelates, monitored by Rhodamine B consumption. Rates, which are shown for M-chelate/O_2 (front) and M-chelate/H_2O_2 (rear) combinations, were monitored by following the UV/Vis absorbance of Rhodamine B over time. These data allow an independent assessment of the relative rate at which diffusible hydroxyl radicals might be generated in the reactions of M-chelate-lisinopril/coreactants/sACE-1, using the same M-chelates and coreactants, under similar conditions. The initial concentrations were 1 µM M-chelate, 10 µM Rhodamine B, 1 mM ascorbate, and 1 mM H_2O_2 (when present). Reactions were performed in a phosphate buffer (pH 7.4) at room temperature. Joyner et al.(2011).[8]

SM References

(1) Sakamoto, Y.; Ishi, T. *J. Mol. Struct.* **1993**, *298*, 129.

(2) Anderegg, G.; Arnaud-Neu, F.; Delgado, R.; Felcman, J.; Popov, K. *Pure Appl. Chem.* **2005**, *77*, 1445.

(3) Martell, A. E.; Motekaitis, R. J.; Chen, D.; Hancock, R. D.; McManus, D. *Can. J. Chem.* **1996**, *74*, 1872.

(4) Furia, T. E. *CRC Handbook of Food Additives*; 2nd ed., 1972; Vol. 1.

(5) Ogino, H.; Ogino, K. *Inorg. Chem.* **1982**, *22*, 2208.

(6) Lau, S.-J.; Kruck, T. P. A.; Sarkar, B. *J. Biol. Chem.* **1974**, *249*, 5878.

(7) Long, E. C. *Acc. Chem. Res.* **1999**, *32*, 827.

(8) Joyner, J. C.; Reichfield, J.; Cowan, J. A. *J. Am. Chem. Soc.* **2011**, *133*, 15613.